Jet Production in Hadron-Hadron Collisions at High Energies

By

Ali Zaman

CIIT/FA09-PPH-001/ISB

PhD Thesis

In

Physics

COMSATS Institute of Information Technology

Islamabad - Pakistan

Spring, 2015

COMSATS Institute of Information Technology

Jet Production in Hadron-Hadron Collisions at High Energies

A thesis presented to

COMSATS Institute of Information Technology, Islamabad

In partial fulfillment
of the requirement of the degree of

PhD (Physics)

By

Ali Zaman

CIIT/FA09-PPH-001/ISB

Spring, 2015

Jet Production in Hadron-Hadron Collisions at High Energies

A Post Graduate Thesis submitted to the Department of Physics as partial fulfillment of the requirement for the award of Degree of PhD in Physics

Name	Registration Number
Ali Zaman	CIIT/FA09-PPH-001/ISB

Supervisor

Prof. Dr. Mais Suleymanov

Advisor, Department of Physics

COMSATS Institute of Information Technology (CIIT)

Islamabad

Final Approval

This thesis titled

Jet Production in Hadron-Hadron Collisions at High Energies

By

Ali Zaman
CIIT/FA09-PPH-001/ISB

Has been approved
For the COMSATS Institute of Information Technology, Islamabad

External Examiner: ______________________________
Prof. Dr. Arshad Majid Mirza (*S.I.*)
Professor, Department of Physics, Quaid-i-Azam University, Islamabad

External Examiner: ______________________________
Dr. Matiullah
Chief Scientist, Physics Division, PINSTECH, Islamabad

Supervisor: ______________________________
Prof. Dr. Mais Suleymanov
Department of Physics, CIIT Islamabad

HoD: ______________________________
Dr. Ahmer Naweed
Department of Physics, CIIT Islamabad

Dean, Faculty of Sciences: ______________________________
Prof. Dr. Arshad Saleem Bhatti (*T.I.*)
CIIT Islamabad

Declaration

I Ali Zaman CIIT/FA09-PPH-001/ISB hereby declare that I have produced the work presented in this thesis, during the scheduled period of study. I also declare that I have not taken any material from any source except referred to wherever due that amount of plagiarism is within acceptable range. If a violation of HEC rules on research has occurred in this thesis, I shall be liable to disciplinary action under the plagiarism rules of the HEC.

Date: ___________________ Signature of the student

____
Ali Zaman
CIIT/FA09-PPH-001/ISB

Certificate

It is certified that Mr. Ali Zaman Registration Number CIIT/FA09-PPH-001/ISB has carried out all the work related to this thesis under my supervision at the Department of Physics, COMSATS Institute of Information Technology, Islamabad and the work fulfills the requirement for award of PhD degree.

Date: ____________________

Supervisor:

____
Prof. Dr. Mais Suleymanov
Advisor
Department of Physics
CIIT Islamabad

Head of Department:

____
Dr. Ahmer Naweed
Associate Professor
Department of Physics
CIIT Islamabad

To My Late Father

ACKNOWLEDGEMENTS

All praises be to the Almighty ALLAH Subhanahu-wa-Ta'aala, the Creator and the Lord of everything alone. Countless blessings, Darood and Salaams on the Last Holy Prophet Hazrat MUHAMMAD SallAllah-o-Alaih-e-wa-Sallam who is Rahmat-ul-lil-Aalameen and is forever a source of guidance and knowledge for humanity and on the all of his Holy Companions Razi-y-Allah-o-Anhum and their True Followers.

I am whole heartedly thankful to my Supervisor Prof. Dr. Sc. Mais Kazim Oglu Suleymanov for his kind supervision, encouragement, guidance, facilitation and cooperation during the whole period of this research work. I am very thankful to Prof. Dr. Mahnaz Haseeb ex-Head of Department and Dr. Farida Tahir for their academic and administrative cooperation. I am also thankful to Dr. Jamila Bashir Butt, Dr. Muhammad Sohail Amjad and Dr. Khusniddin Olimov for their guidance and help. I am also obliged to Prof. Dr. Arshad Saleem Bhatti (TI), Dean Faculty of Sciences, Prof. Dr. Sadia Manzoor, Head, and Dr. Ahmer Naweed, Associate Head, Department of Physics and other faculty and staff members of the Department of Physics, for the valuable support and coordination in their respective fields. I am grateful to them for their cooperation during the period of my study at COMSATS Institute of Information Technology Islamabad.

Special thanks to Higher Education Commission (HEC) Government of Pakistan, for financial support by awarding me the scholarship under Indigenous5000 PhD Scholarship Program Batch-IV which made possible to continue and complete my higher studies.

I am thankful of my senior coworkers Dr. Muhammad Ajaz and Dr. Kamal Hussain Khan for their kind cooperation, my fellows and friends Dr. Waqar Mahmood, Dr. Imran Khan, Obaidullah Jan and Akhtar Iqbal Khattak for their nice and unforgettable company at CIIT Islamabad, especially Dr. Shakeel Mahmood for his very nice cooperation who also made me easy to reach home most of the evenings. I cannot forget precious moral support from my dear friends, Muhammad Noaman ul Haq, Syed Ihsan Hyder, Muhammad Shoaib Kamran and Dr. Abdul Jabbar Bhutta and especially Haroon Rashid whose kind and nice cooperation is really unforgettable. My thanks are due to all those who supported me in any way and at any stage of my studies.

I am extremely thankful to my Sisters, and Brothers Maulana Shams-uz-Zaman and his family, Dilbar Hussain, Bashir and his family, and specially Noor Zaman and his family and Saif-ur-Rahman, for their kindness, prayers, cooperation and every kind of support. I am also thankful to my wife, who joined me in the start of this writ-up, for her help and prayers. May Almighty ALLAH shower his countless blessings on my Late Father, and my Mother, her kindness and prayers are the keys of my successes.

Ali Zaman

CIIT/FA09-PPH-001/ISB

ABSTRACT

Jet Production in Hadron-Hadron Collisions at High Energies

We investigated the effects of jet production on the following parameters: multiplicity, pseudorapidity, transverse momentum and transverse mass distributions of charged particles produced in hadron-hadron collisions at 1.8 TeV, centre of mass energy, using the Dubna version of HIJING model. These distributions are analyzed for the whole range and for six selected regions of the polar angle (angle of the secondary particles with respect to the beam axis) as a function of number of jets. The results for the charged particles multiplicity distributions were compared with experimental ones coming from the SPS and Tevatron experiments and the increase in the multiplicity of the charged particles influenced by multi-jet events is discussed. The results for pseudorapidity distributions are interpreted and discussed in connection to the increase observed in the multiplicity of charged particles as a result of its multi-jet dependence and are also discussed in comparison with the experimental results coming from the CDF Collaboration. The analysis of effect of the multi-jet events on the transverse momentum and transverse mass distributions is also discussed in connection to the increase in the multiplicity and pseudorapidity density of charged particles. We concluded that high multiplicity regions, the increased pseudorapidity density and the high p_T regions correspond mainly to the multi-jet events.

TABLE OF CONTENTS

LIST OF FIGURES

LIST OF TABLES

LIST OF ABBREVIATIONS

AA	Nucleus-Nucleus
ALICE	A Large Ion Collider Experiment (http://alice-collaboration.web.cern.ch)
AuAu	Gold-Gold
BNL	Brookhaven National Laboratory (http://www.bnl.gov)
CDF	Central Detector at Fermilab (http://www-cdf.fnal.gov)
CERN	European Centre for Nuclear Research (http://www.cern.ch)
CMS	Centre-of-Mass System
dAu	Deuteron-Gold
DESY	Deutsches Elektronen-Synchrotron (http://www.desy.de)
DGLAP	Dokshitzer-Gribov-Lipatov-Altarelli-Parisi
DIS	Deep-Inelastic Scattering
E735	Experiment735 at Tevatron Fermilab
E_T	transverse energy
fm	femto-meter (10^{-15}m)
FORTRAN	Formula Translation
GeV	Giga electron Volt (10^9 eV)
H1	H1 (http://www.desy.de)
HERA	Hadron-Electron Ring Accelerator (http://www.desy.de)
HERWIG	Hadron Emission Reactions with Interfering Gluons (http://hepwww.rl.ac.uk/theory/seymour/herwig/)
HIJING	Heavy Ion Jet Interaction Generator (http://www-nsdth.lbl.gov/~xnwang/hijing/)
HIJSET	a HIJING's subroutine
IHPR2(8)	HIJING parameter for Number of Jets

ISR	Intersecting Storage Ring (http://www.cern.ch)
KNO	Koba-Nielsen-Olesen
LAB	Laboratory (Fixed Target Experiment)
LEP	Large Electron–Positron Collider (http://www.cern.ch)
LHC	Large Hadron Collider (http://www.cern.ch)
LO	Leading-Order
LPHD	Local Parton-Hadron Duality
MC	Monte Carlo
MD	Multiplicity Distribution
MeV	Mega electron Volt (10^6 eV)
m_T	Transverse Mass
NB	Negative Binomial
N_{ch}	Multiplicity of Charged Particles
N_{jet}	Number of Jets
NLO	Next-to-Leading Order
NMF	Nuclear Modification Factor (R_{AA})
OPAL	Omni-Purpose Apparatus for LEP (http://opal.web.cern.ch/Opal)
pA	Proton(or Hadron)-Nucleus
Pb–Pb	Lead-Lead
PDFs	Parton Distribution Functions
PETRA	Positron Electron Tandem Ring Accelerator (http://www.desy.de)
PHOJET	PHOJET (http://www-ik.fzk.de/~engel/phojet.html)
pp	Proton-Proton (or Hadron-Hadron)
pQCD	Perturbative Quantum Chromodynamics
p_T	Transverse Momentum

PYTHIA	PYTHIA (http://home.thep.lu.se/~torbjorn/Pythia.html)
QCD	Quantum Chromodynamics
QGP	Quark-Gluon Plasma
RHIC	Relativistic Heavy Ion Collider (http://www.bnl.gov)
SLAC	Stanford Linear Accelerator Centre (http://www-ssrl.slac.stanford.edu)
SM	Standard Model
SPEAR	Stanford Positron Electron Asymmetric Ring (http://www-ssrl.slac.stanford.edu)
SPS	Super Proton Synchrotron (http://www.cern.ch)
TeV	Tera electron Volt (10^{12} eV)
TMD	Transverse-Momentum Dependent
UA5	UA5 (an experiment at SPS)
ZEUS	ZEUS (http://www.desy.de)
η	Pseudorapidity

Chapter 1 Introduction

Particle physics is aimed to address the study of the ultimate constituents of matter and the basic forces through which these constituents interact with each other.

The fundamental constituents of matter are the fermions (carrying spin ½) and the mediators of interactions between them are bosons (carrying integral spin). The four fundamental interactions in nature are the following. The strong interaction with gluons (*g*) as mediator bosons and the particles that interact through this interaction are those which possess the color charge and these are the only quarks. The weak force with W (W^+, W^-) and Z^0 bosons as mediators, leptons and quarks are the participating particles in this interaction, and this is the only force responsible for the neutrinos' interactions. The electromagnetic force having photon (γ) as mediator boson, which is responsible for the interactions of electrically charged particles. The force of gravity whose mediator boson is the graviton which is not discovered yet, the objects possessing mass interact through this force. The effects of the gravity on the particles are negligible as compared to the effects of other three forces [1, 2].

In the standard model (SM) of particle physics the building blocks of the matter are the quarks and the leptons which are grouped in three generations on the basis of their masses interacting through the two forces; the electroweak force (which is the unified form of the electromagnetic and the weak force) and the strong force, and the gravity is not included in this framework [1, 2]. All the predictions of the SM has been completely tested and discovered experimentally during last ~50 years, the last of this was the remarkable discovery of the Higgs boson at the large hadron collider (LHC) CERN in 2012. Figure 1.1 shows a schematic arrangement of fundamental particles and forces included in the SM framework.

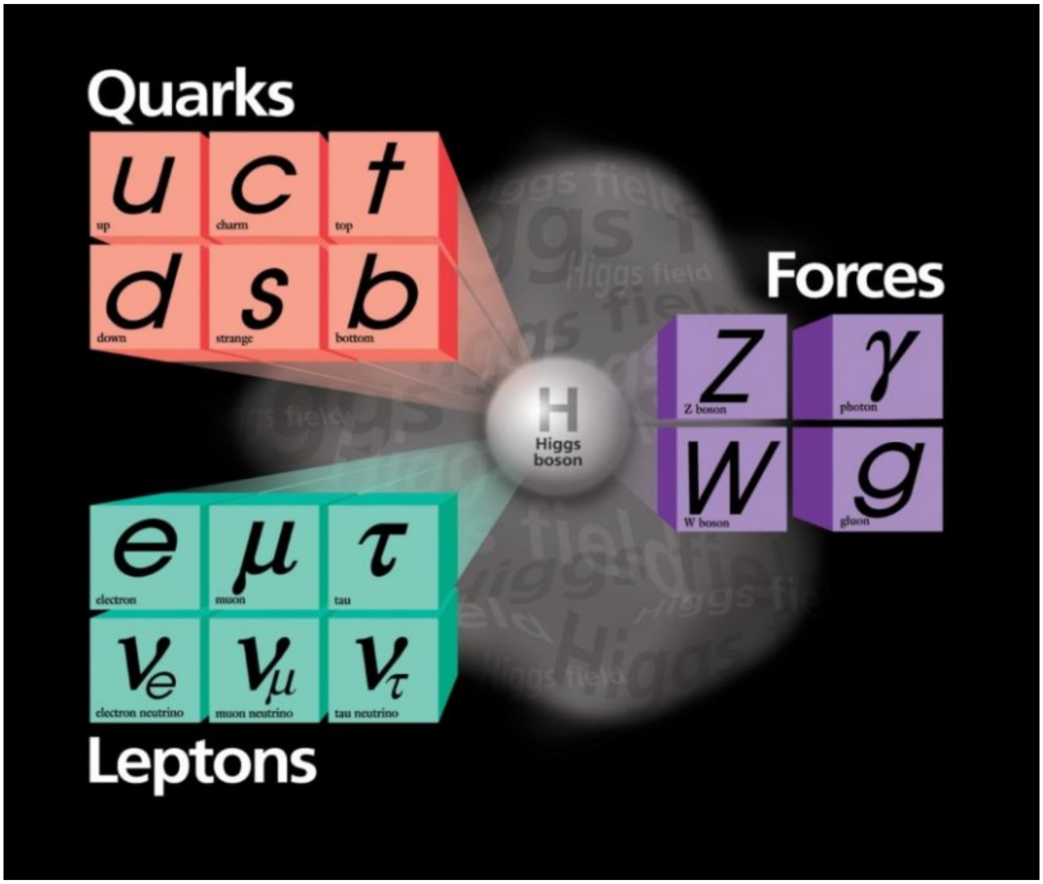

Figure 1.1 Fundamental particles and forces in the framework of SM of particle physics [3]

Physics of high energy hadronic collisions reveals the properties of strongly interacting matter like hadrons and their constituents, quarks which interact via gluons. In relativistic and ultrarelativistic hadronic interactions, the nucleons breakup at such high energies and lose their individual identity. During such interactions free quarks and gluons are produced at a very short time scale ~10^{-24} sec and thus a new state of strongly interacting matter; the quark-gluon plasma (QGP) is created [4, 5]. These free quarks hadronize by interacting with other quarks and anti-quarks to produce hadrons either combining in a doublet state of quark-antiquark pair $q\bar{q}$ the mesons or in quark triplet state qqq termed as the baryons.

The theory of strongly interaction or the quantum theory of the color (chrome), the quantum chromodynamics (QCD), forbids the individual existence of quarks and they are confined in the hadrons. During the process of formation of hadrons from the quarks, these particles may assume the form of a cone, which is termed as jet production. By studying the properties of these jets we can get information about the properties of quarks [1, 2, 4, 5].

In the present work we study the effects of the jet production on different parameters of the charged particles produced in hadron-hadron collisions, at energy 1.8 TeV in the frame of centre-of-mass system (CMS), using Dubna version of the heavy ion jet interaction generator (HIJING) Monte Carlo model for event simulations.

Layout of this Thesis

First chapter of this thesis is a general introduction. Second chapter is about brief description/review of the jets in high energy physics. The methodology is described in third chapter which includes the procedure of this research work and a general description of the HIJING Model. A detailed discussion of the results for different parameters of charged particles produced in pp collisions is presented in chapter 4. Finally conclusions are summarized in chapter 5.

Chapter 2 Jets in High Energy Collisions

This chapter contains a brief description about the jets, their production, quenching and importance in high energy hadronic collisions.

2.1 Jets

The word jets employed (and first used by D. H. Perkins in 1954) to describe the collimation of the secondary hadrons produced in high energy collisions. A jet results from the fact that the average transverse momentum of the secondaries is of the order of a few GeV/c, being determined by the range of the strong interaction. In a high energy collision, the secondaries will generally carry large longitudinal momentum components and therefore emerge in a narrow cone [1].

In high energy hadronic collisions, jets are defined as a narrow cone of hadrons or other particles produced by the hadronization of quarks or gluons, collectively termed as partons. Due to the quantum chromodynamics (QCD) color confinement, particles with a color charge, like quarks, cannot exist in free state. Therefore, in a high energy collision, they form jets which fragment into hadrons before their direct detection. The process of the formation of colorless hadrons out of the colored partons (quarks and gluons) is known as hadronization. In a particle collider experiment, the process of hadronization occurs at high energy collisions where free quarks and gluons are created. Due to the color confinement, these quarks and gluons combine with quarks and antiquarks, which are created spontaneously from the vacuum and ultimately form the colorless hadrons. To determine the properties of the original quark, these jets must be measured and analyzed in a particle detector [1, 2, 4—9].

2.2 Importance of Jets

In particle physics jets are of great importance because these provide explanation and understanding about the observation of grouped/shower particles in a collider detector experiment. These jets are the experimental evidence of the existence of the quarks in the hadrons, and properties of these jets reflect the properties of the quarks from which these jets are originated. Jet physics also provides the details about the hadronization of the colored partons: quarks or gluons and their fragmentation into colorless hadrons.

Jets are considered as a hard probe to get the information about the new states of the strongly interacting matter. So the study of the jet production in high energy hadron-hadron collisions is of great interest and importance. Within the frame of the quantum chromodynamics QCD - the theory of strong interaction, jets are believed to result from quarks and gluons with high transverse momentum (p_T) [1, 6], and thus should carry information about the deconfined state of the strongly interacting matter [1, 2, 4—7], supposedly produced in such high energy interactions. First time it was proposed by Hagedorn that there should be some critical temperature for hadrons after which the hadrons transform to the system of free quarks and gluons [10]. Analyzing the energy spectrum of the hadrons he found the critical temperature to be around ~200 MeV. In framework of the QCD this phenomena is called deconfiment.

Jets produced in high energy heavy ion interaction are important because the initial hard scattering is a natural probe for the QCD matter created in this high energy collision indicating its phase. When the formation of quark-gluon plasma (QGP) [4, 5, 11, 12] occurs by phase crossover of the QCD matter there is significant growth of the radiative energy loss in the medium. This energy loss in the medium quenches the outgoing jet [4, 11] effectively. Different phases of the strongly interacting QCD matter are shown in Figure 2.1.

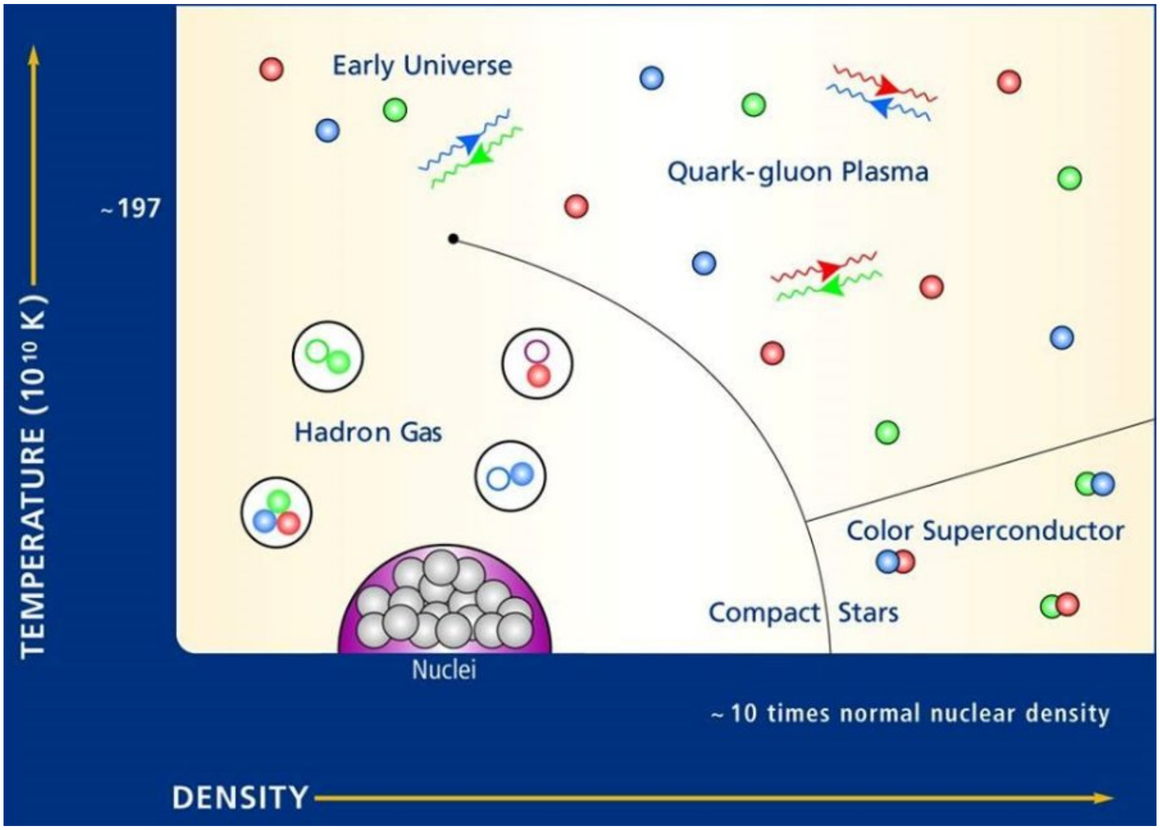

Figure 2.1 Phases of the strongly interacting matter [13]

2.3 Jet Production

Jet production occurs in high energy collisions during QCD hard scattering processes when the partons, quarks and gluons are created with high transverse momentum (p_T). A pictorial view of a hard scattering event is shown in Figure 2.2 and the schematic of the different stages of the jet production in $pp(\overline{p})$ interaction is presented in Figure 2.3, which describes the steps of the jet evolution from the hard scattering of quarks, hadronization process and finally their calorimetric measurements.

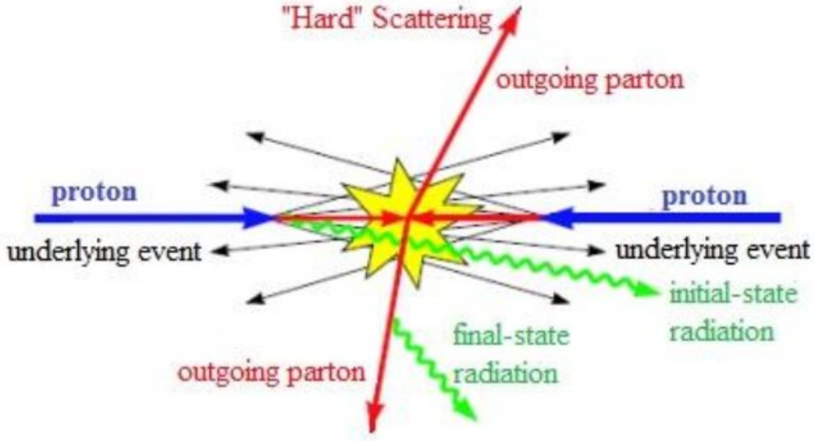

Figure 2.2 Hard scattering event in pp collision, a pictorial view [14, 16]

The jet production cross-section is used to describe the probability for the creation of a certain set of jets in a collision. This cross-section is described by the parton distribution functions (PDFs) and is the average of an elementary pQCD quark, antiquark, or gluon process. In a two particle scattering the process of production of the most frequent jet pair, the cross-section of jets production in a hadronic collision [14, 15] is given by the following equation.

$$\sigma_{ij\to k} \quad \sum_{i,j}\int dx_1 dx_2 d\hat{t} f_i^1\left(x_1, Q^2\right) f_j^2\left(x_2, Q^2\right)\frac{d\hat{\sigma}_{ij\to k}}{d\hat{t}} \tag{2.1}$$

where, x is the longitudinal momentum fraction; Q^2 the transferred momentum; $\sigma_{ij\to k}$ the perturbative QCD cross-section for the process $ij\to k$; $f_i^a\left(x_a, Q^2\right)$ the parton distribution function for finding particle species i in beam a, and ?s are the elementary cross-sections.

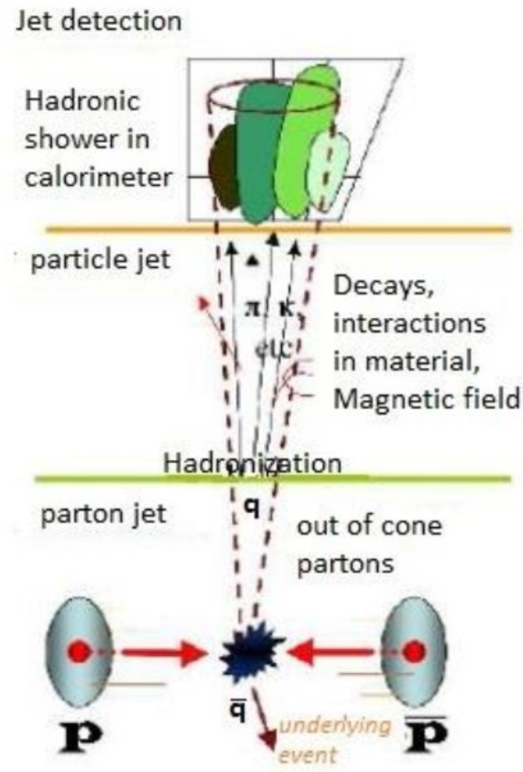

Figure 2.3 A schematic representation of the different stages of the jet production and its measurements [14]

2.4 Jet Fragmentation

In the perturbative QCD calculations there may be colored partons in the final state, but experimentally there observed only the colorless hadrons produced by these partons. To describe the experimental observation resulted from a given interaction in a detector, all of the exiting colored partons must undergo the process of parton showering firstly and then these produced partons combine to form hadrons. In a high energy collision, the process of formation of hadrons, soft QCD radiation, or both of these processes [8, 12], are termed as fragmentation or hadronization.

When a parton, produced in a hard scattering, exits the interaction, there will be an increase in the strong coupling constant with the separation. This results an increase in the probability of the QCD radiation, which is shallow-angled with respect to the initial parton predominantly. So a parton will radiate gluons, which will be resulted in production of quark-antiquark ($q\bar{q}$) pairs and so on. The generated each new parton is nearly collinear with its parent. By convolving the spinors with fragmentation functions $P_{ji}\left(\frac{x}{z},Q^2\right)$, this can be described in a way similar to that of the of PDFs evolution. Which can be described by Dokshitzer-Gribov-Lipatov-Altarelli-Parisi (DGLAP) equation [17] given below,

$$\frac{\partial}{\partial \ln Q^2} D_i^h\left(x,Q^2\right) \quad \sum_j \int_x^1 \frac{dz}{z} \frac{\alpha_S}{4\pi} P_{ij}\left(\frac{x}{z},Q^2\right) D_i^h\left(z,Q^2\right) \tag{2.2}$$

The parton showering results in the production of low energy partons successively, and thus it exits the pQCD validity region. When the parton showers are formed then to describe the length of time the phenomenological models should be applied. And then these colored partons are combined into their confined state i.e. the colorless hadrons.

2.5 Jet Finding Procedures

Due to the color confinement of the quarks and gluons their final state distribution cannot be directly measured, because the hard scattering final state contains colorless hadrons only. In the jet defining algorithms, the observed hadrons and the partons in the final state of the high energy hadronic interactions are associated to the local parton-hadron duality (LPHD) [18] correspondence. Satisfaction of the LPHD correspondence implies that jet production can be used as tool for mapping the observed long-distance hadronic final state onto underlying short-distance partonic states [19].

Jet finding algorithms define a functional mapping between the particles in terms of their kinematic descriptions (e.g. momentum etc.) and the jet configurations, represented by suitable jet variables.

$$particles \xrightarrow{jet-a\lg orithm} jets$$

Ideally, a jet defining algorithm should be [19, 20]:

- Fully specified in terms of completely defining the procedure, the kinematical variables and the variety of corrections must be specified in a unique way.
- It should be well behaved theoretically i.e. the jet algorithm must be collinear and infrared safe, do not use any ad-hoc parameter.
- It should be detector independent in terms of the type, segmentation or size of the detector.
- The algorithm should be consistent so that it must have equal applicability for the theoretical and experimental level.

Every algorithm must satisfy the first two criteria as the LPHD can only be fulfilled if the algorithm obeys the infrared safety condition. That makes sure the insensitivity of outcome on the emitted collinear or soft partons. Probably, the last two criteria totally cannot be satisfied, as the experimental apparatus dependencies cannot be removed completely.

2.6 Jets Kinematics

Generally the interacting partons are not in the centre-of-mass system (CMS) frame of the collision system, as there is event to event variation in the fraction of momentum carried by the partons. The partonic centre-of-mass system is therefore boosted along the direction of the colliding hadron randomly, so that the jets can be described conveniently in terms of the following longitudinally boost-invariant variables [19]:

Mass $$m \quad \sqrt{E^2 - p_x^2 - p_y^2 - p_z^2} \qquad (2.3)$$

Transverse momentum $$p_T \quad \sqrt{p_x^2 + p_y^2} \qquad (2.4)$$

Azimuthal angle $$\varphi = tan^{-1}(p_y/p_x) \qquad (2.5)$$

Rapidity $$y \quad \tfrac{1}{2}\ln\left(\frac{E + p_z}{E - p_z}\right) \qquad (2.6)$$

where E is total energy of secondary particles and p_z is their longitudinal momentum along z-axis.

For the relativistic limit, when $p >> m$, conveniently the quantities which are directly measurable are: the transverse energy ($E_T = E\ Sin\ \theta \approx p_T$), the azimuthal angle ($\varphi$) and the pseudorapidity η given by,

$$\eta \quad -\ln[\tan(\theta/2)] \tag{2.7}$$

where the polar angle θ (with the beam axis) is given by,

$$\theta = tan^{-1}(p_T/p_z) \tag{2.8}$$

2.7 Jet Algorithms

Jet algorithms can be classified in two fundamental classes: the recombination/sequential or clustering algorithms [21-25] and cone algorithms [26-29]. These algorithms use the assumptions that hadrons being associated with a jet should be 'nearby' each other. To define a jet, in cone jet algorithms are based on vicinity in real space including angles, while the sequential algorithms are based on vicinity in momentum space and thus known as k_T algorithms.

- The sequential or k_T algorithms are inspired by parton showering processes in QCD [14, 21, 22, 30]. These algorithms simulate the processes of the hadronization backward and group the pairs of particles in increasing order of p_T successively.
- The cone algorithms are designed for jets in the hadronic interactions. All particles are grouped inside a cone of radius R in $\eta \times \varphi$ space to form a single jet [26, 27, 31]. The radius of cone is defined as $R \quad \sqrt{(\Delta\eta)^2 + (\Delta\phi)^2}$, where $\Delta\eta$ and $\Delta\varphi$ are the particle or parton separation in pseudorapidity and azimuthal angle (measured in radians) with respect to axis of the jet.

2.8 Experimental Observation of the Jets

First experimental observation of the jets, as an evidence of the quarks inside hadrons, was in electron-positron annihilation to hadrons at Stanford positron electron asymmetric ring (SPEAR), Stanford Linear Accelerator Centre (SLAC) [32—35] at beam energy ~7 GeV in 1975 and then at positron electron tandem ring accelerator (PETRA), deutsches elektronen-synchrotron (DESY) [36—42] at beam energy ~30 GeV in 1979. The angular distribution analysis of this quark initiated two-jet event showed that these hadron jets are associated with the spin ½ quarks constituents [1, 37—42]. This two-jet event, illustrated in Figure 2.4, can be regarded as a two step process, an electromagnetic process $e^+e^- \to q\bar{q}$ to produce quark-antiquark pair and then fragmentation of this $q\bar{q}$ pair to two hadronic jets [1, 36].

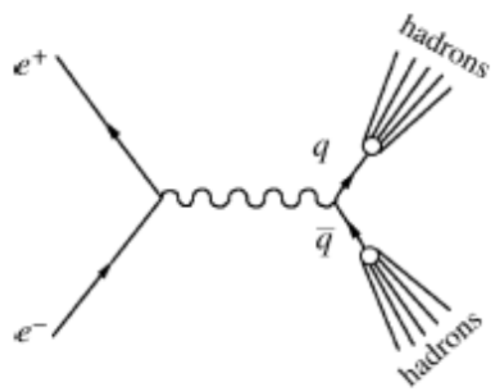

Figure 2.4 Production mechanism of two-jets in e^+e^- annihilation to hadrons [36]

The gluon-initiated jets were also observed in e^+e^- collider at PETRA which resulted by the emission of a high-momentum gluon by quark or antiquark before their fragmentation and then these three $q\bar{q}$ pair and the gluon hadronize to form 3-jets of hadrons [1, 36, 41, 42]. A schematic of this three-jet event is shown in Figure 2.5.

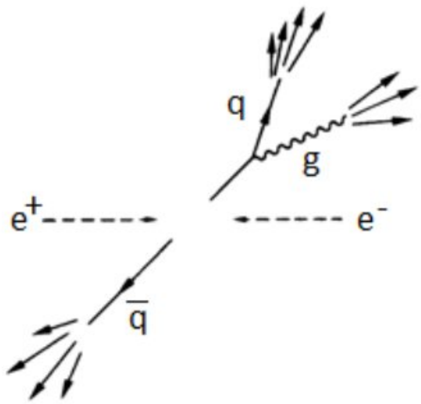

Figure 2.5 Production mechanism of a three-jet event in the process $e^{+}e^{-} \rightarrow q\bar{q}g \rightarrow hadrons$ [1].

Such type of hadronic jets have been observed in different kind of interactions like electron-positron collider at large electron–positron collider (LEP) [43—45] and $p\bar{p}$, *pp, pA* and *AA* collisions at various range of colliding energies (at intersecting storage ring (ISR) [46], super proton synchrotron (SPS) [47], Tevatron Femilab [14, 48—50], relativistic heavy ion collider (RHIC) [51, 52] and the largr hadron collider (LHC) [14, 19, 53], which provided strong evidence about the existence of quarks inside the hadrons.

A schematic of different stages of the jet production in a $pp/p\bar{p}$ collisions is shown in Figure 2.3 and following Figure 2.6 is an art picture of the jet production in hadron-hadron collisions. And Figure 2.7 interprets the kinematics of parton scattering during jet production at a proton-antiproton collider, where P1 and P2 are momenta of the colliding proton and antiproton respectively being carried by the interacting partons (quarks or gluons) and P3 and P4 are the observed 4-momenta of the outgoing partons being fragmented to two jets of secondary hadrons [1].

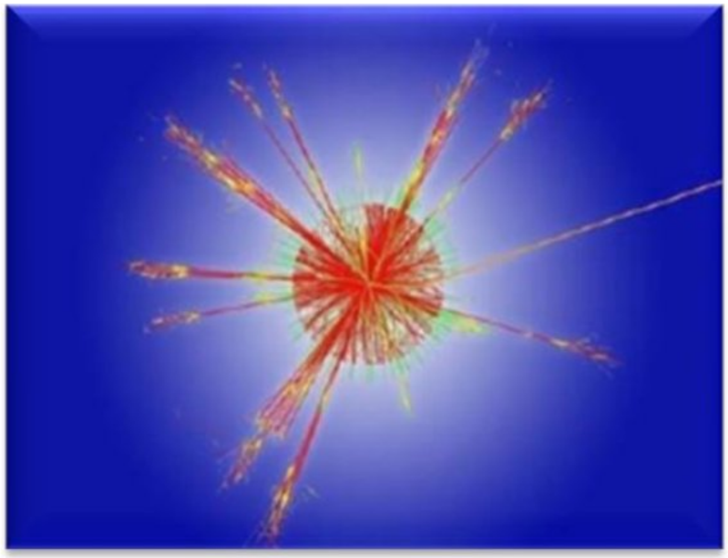

Figure 2.6 An art picture of jets in *pp*-collisions [54]

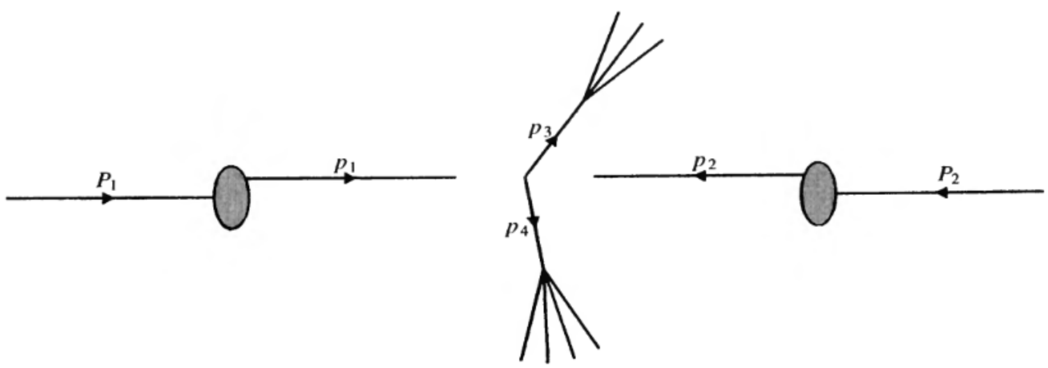

Figure 2.7 Schematics of parton-parton interaction for jet production in a $pp/p\bar{p}$ collision [1]

Jets in *ep* Collisions

The observation of jet production at hadron-electron ring accelerator (HERA) tested the theory of strong interactions, quantum chromodynamics (QCD), and extracted information on the parton content of the proton and of real or virtual photons [55]. QCD predicts the production of partons with large transverse momentum, fragmenting into jets with similar four-momentum. The study of jet observables therefore allows the investigation of the underlying parton dynamics. Perturbative QCD predictions, however, also need the parton content of the proton and photon as input. Jet cross-section can thus be used to further constrain the partons density functions (PDFs) obtained by global fits.

The clustering of final state objects into a few jets is performed by applying a jet finding algorithm. The H1 [56] and ZEUS [57] collaborations presented the results obtained with the k_T algorithm. This algorithm has the advantage of being infrared and collinear safe and to be minimally sensitive to fragmentation and underlying event effects. Correction of reconstructed data is performed from detector to hadron level using a full detector simulation. Next-to-leading order (NLO) QCD predictions are corrected from parton to hadron level. This involves the fragmentation of partons into hadrons and secondary interactions between partons of the photon and proton remnants. Correction factors are obtained from leading-order (LO) Monte Carlo (MC) models where NLO effects are modeled by QCD cascades.

In LO two types of processes are distinguished. In direct processes the exchanged photon interacts as a whole with the proton and produces jets. In resolved interactions, the photon is treated as a source of partons, one of which produces a hard scattering with the proton, leaving behind a soft photon remnant. The concept of resolved photons is useful in photoproduction as well as in deep-inelastic scattering (DIS) when $E_T^2 >> Q^2$, where E_T is the transverse energy of the partons produced in the hard interaction and Q^2 is the virtuality of the exchanged photon. To separate direct and resolved enhanced event samples, the momentum fraction of the photon entering the hard scattering, x_γ, can be used. On hadron level, the variable x_γ^{jet}, which is correlated to the parton level x_γ, is calculated as $x_\gamma^{jet} \quad \sum_{jets} E_T^{jet} e^{-\eta^{jet}} \big/ 2E_\gamma$, where E_T^{jet} and η^{jet} are the jet transverse energy and pseudorapidity and E_γ is the energy of exchanged photon.

Using QCD factorization, the direct and resolved cross-sections for producing N jets, integrated over phase space, can be expressed as [55],

$$\sigma_{direct}^{ep \to e+Njets+X} \quad \int_{\Omega} d\Omega f_{\gamma/e}\left(y, Q^2\right) \sum_{i} f_{i/p}\left(x_p, \mu_p^2\right) \sigma^{\gamma i \to Njets} \tag{2.9}$$

$$\sigma_{resolved}^{ep \to e+Njets+X} \quad \int_{\Omega} d\Omega f_{\gamma/e}\left(y, Q^2\right) \sum_{ij} f_{i/p}\left(x_p, \mu_p^2\right) f_{j/\gamma}\left(x_\gamma, \mu_\gamma^2\right) \sigma^{\gamma i \to Njets} \tag{2.10}$$

where $f_{\gamma/e}$, $f_{i/p}$ and $f_{j/\gamma}$ are flux factors for photons originating from the electron and for partons originating from the proton and the photon, respectively, evaluated at given fractional momentum-energies and factorization scales. The partonic cross-sections $\sigma^{\gamma i \to Njets}$ and $\sigma^{ij \to Njets}$ can be calculated in LO and NLO as a function of strong coupling constant $\alpha_S \mu R$, where μR is the renormalization scale. The choice of renormalization and factorization scales will lead to some uncertainty in the predicted cross-sections. Different NLO calculations further differ mainly in their treatment of infrared and collinear divergences.

The H1 [56] and ZEUS [57] collaboration have measured jet production in *ep* collisions with real and virtual photons in a large kinematic range. They obtained cross-sections with high accuracy which falls over more than six orders of magnitude as a function of transverse energy. The obtained values of the strong coupling constant α_S are in agreement with the current world average.

Next-to-leading order QCD calculations describe the jet cross-section in a better manner, with exceptions for forward jets at low momentum transfer Q^2 and E_T^{jet} and for the direct to resolved ratio of enhanced components in dijet production events.

Di-Jet in Photon-Photon Collisions

The omni-purpose apparatus for LEP (OPAL) collaboration studied di-jet production in interactions of quasi-real photons (carrying only a small four-momentum $Q^2 \approx 0$) emitted by electron beams at e^+e^- collider at $\sqrt{s_{ee}}$ = 161 and 172 GeV centre-of-mass energies [58]. They used the cone jet algorithms for the reconstruction of jets. They studied the angular distribution of direct and double-resolved events and compared with the LO and NLO pQCD predictions. They measured cross-section for inclusive two-jet production as a function of E_T^{jet} and $|\eta^{jet}|$ and compared with the calculations of NLO pQCD. The cross-section for inclusive two-jet processes as a function of $|\eta^{jet}|$ was also compared with the PHOJET and PYTHIA Monte Carlo predictions [59], calculated by using the parameterizations of the parton distributions of photons. The underlying event influences were also studied in order to reduce the modal dependence of the Monte Carlo predicted cross-section.

Inclusive one-jet and two-jet production cross-section in photon-photon collision was previously calculated at Tristan e^+e^- collider at $\sqrt{s_{ee}}$ = 58 GeV centre-of-mass energy [60] and at LEP e^+e^- collider at $\sqrt{s_{ee}}$ = 130 and 136 GeV centre-of-mass energy [61].

In the cone jet defining algorithms the total transverse energy E_T^{jet} of the jets is the scalar sum of the transverse energy of their components within the cone [61]. The transverse energy E_{Ti} of an i^{th} particle with respect to the z axis of the detector, is defined as $E_{Ti}=E_i Sin\theta_i$. For an acceptable cone jet, the value of E_T^{jet} should be greater than a minimum energy $E_T^{\min}$ certainly. The cone jet algorithms results depend on $E_T^{\min}$ and the cone size (radius of cone) $R \quad \sqrt{(\Delta\eta)^2+(\Delta\phi)^2}$ with pseudorapidity $\eta \quad -\ln[\tan(\theta/2)]$ and azimuthal angle φ.

The OPAL Collaboration also studied the jet's internal structure in photon-photon collisions at the hadronic level. The shape of a jet is characterized by the fractions of transverse energy of jet (E_T^{jet}) which resides inside the inner cone of radius r being concentric with the jet defining cone [58]:

$$\psi(r) \quad \frac{1}{N_{jet}}\sum_{jets}\frac{E_T(r)}{E_T(r \quad R)} \tag{2.11}$$

where $E_T(r)$ is the jet's transverse energy inside the inner cone with radius r and N_{jet} is the total number of jets. By definition, $\psi(r=R) = 1$.

Multi-Jet Final States

Multi-jet production have been investigated in hadronic final states at HERA and Tevatron colliders, which will also play a central role for physics at the large hadron collider (LHC) [62]. The experimental data for such hadronic final states can be interpreted by perturbative calculation for multi-jet production and by the parton-shower Monte Carlo event simulations. PYTHIA [59] and HERWIG [28], based on the collinear evolution of jets in the initial-state are used to reconstruct the exclusive processes, excluding the finite-k_T contribution that corresponds to implementation of the corrections to the transverse momentum ordering in the parton branching algorithm.

At the LHC, experimental analysis of such multi-jet final states relies on the realistic parton-showers Monte Carlo simulation. Investigation of production of multi-particles at the LHC qualitatively acquires some new features compared to the previous hadron collider experiments due to opening up of the large phase space for events characterization. That will bring in both potentially large radiative corrections and the new effects in the non-perturbative components of the processes being probed near boundaries of the phase-space [62].

F. Hautmann and H. Jung described the k_T-dependent Monte Carlo showers method [62], which is based upon transverse-momentum dependent (TMD) parton distribution and the matrix elements being defined in high-energy factorizations. This method is advantageous over the standard Monte Carlo generators mainly due to including the corrections to collinear-ordered shower, and inclusion of QCD coherence effects associated with finite-angle radiations from space-like parton that carries the soft longitudinal momentum arbitrarily. Sensitivity to these dynamical features is bound to be enhanced by the high-energy multi-scale kinematics. On the theoretical background of this k_T-showers method one can go to arbitrarily high transfer-momentum scale, and thus making it feasible for jet physics event simulation at the large hadron collider. The k_T-dependent shower method [62] can be fully used up to high transfer-momentum scale.

2.9 Jet Quenching

Among the other tools like hadronic radiations, electromagnetic radiations, dissociation of the quarkonium states etc. jet quenching is also an important probe to study the properties of QGP [4, 5]. Jet quenching is the result of the energy loss by jets in the medium at partonic level of interactions due to medium induced gluon radiations [4, 63—65]. In order to study the suppression of the high p_T jets, the nuclear modification factor (NMF) (R_{AA}) is usually used. The NMF is defined as the ratio of the yield of particles in nucleus-nucleus collisions to that in the *pp* collisions and normalized to the N_{coll}.

$$R_{AA}(p_T) \quad \frac{1}{\langle N_{coll} \rangle_C} \times \frac{d^2 N_{AA}^C / dp_T d\eta}{d^2 N_{pp} / dp_T d\eta} \tag{2.12}$$

where $d^2N^c_{AA}/dp_Td\eta$ and $d^2N_{pp}/dp_Td\eta$ are the differential cross sections of secondary charged particles produced in central nucleus-nucleus and pp-interactions respectively at the same energy. $\langle N_{coll} \rangle_c$ is a number of participant nucleons in the central nucleus-nucleus events [66].

Experimental measurements recorded at RHIC [67—71] and LHC [67, 72—83] strongly supports the existence of the QGP. Observation of the jet quenching has been reported by experiments at the RHIC [67, 84—93] and at the LHC [68, 82, 83, 94—105] by measuring the production of high p_T jets and some other observables. A large ion collider experiment (ALICE) Collaboration at the LHC has recently reported their results for the measurement of jet suppression in central lead-lead (Pb–Pb) collisions at $\sqrt{s_{NN}} \quad 2.76$ TeV [67].

For *pp* collisions the jet is being determined by production of the high p_T hadrons and in general this is balanced by the production of another high p_T hadrons jet in the opposite direction. In case of the nucleus-nucleus (*AA*) collisions, if the primary hard scattering occurs near the edge of the reaction region, the balancing jet has to encounter the dense and hot nuclear medium mostly and thus being quenched [4]. A schematic illustration of this effect is shown in Figure 2.8 below.

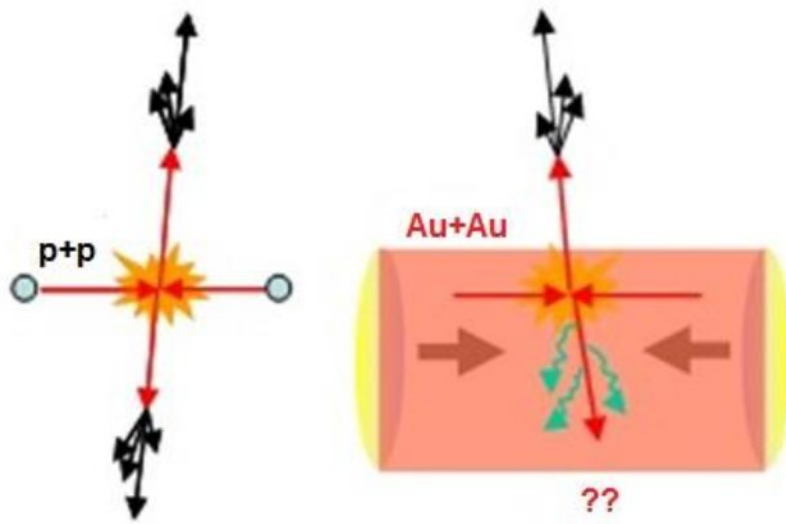

Figure 2.8 A pictorial representation of jet production in pp collisions (left) and jet production/quenching in nucleus-nucleus (*AA*) (particularly gold-gold (*AuAu*)) collisions (right) [106]

The RHIC at brookhaven national laboratory (BNL) reported the study of azimuthal distribution of jet production in gold-gold (*AuAu*), deuteron-gold (*dAu*) and proton-proton (*pp*) collisions at $\sqrt{s}$ = 200 GeV [4]. Considering the azimuthal angle of the near-side hadronic jet to be zero degree, the balancing (away-side) hadronic jet can be clearly observed, both in *pp* and *dAu* collisions, at 180°. For the case of *dAu* collisions, the balancing jet traverses the nuclear medium but there is no significant quenching effect as this *dAu* contains normal nuclear matter. Where as, in the case of *AuAu* collisions strong suppression of the balancing jet is clearly observed [4, 85, 107, 108]. These results are shown in Figure 2.9.

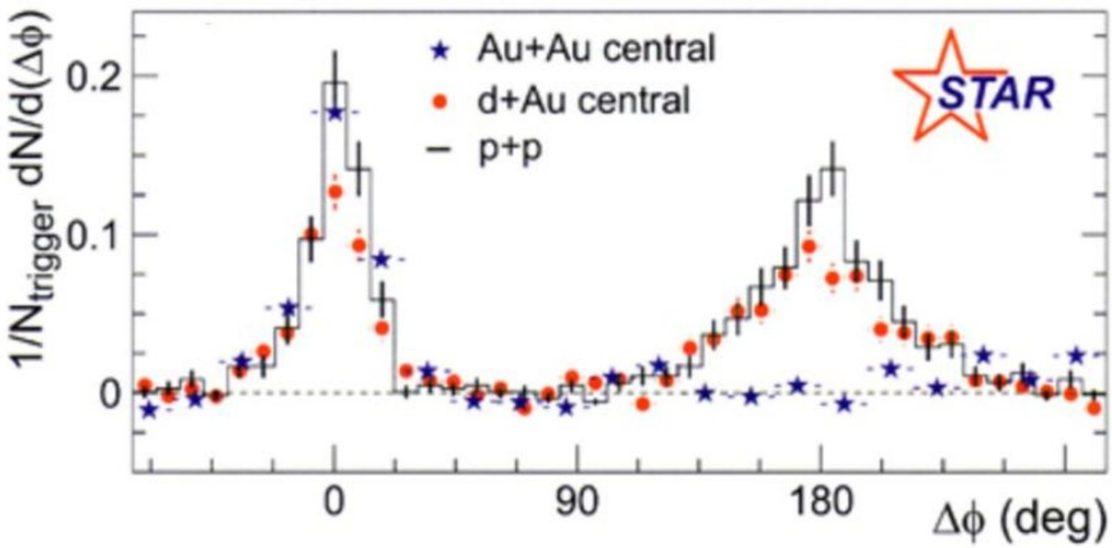

Figure 2.9 Azimuthal angular distributions of the hadrons produced in gold-gold (AuAu), deuteron-gold (dAu) and proton-proton (pp) collisions [4, 85, 107, 108]

Chapter 3 The Method

In this chapter the methodological procedure for the study of effect of jet production on different parameters of charged particles produced in hadron-hadron collisions at high energy, is briefly described and a detailed and brief description of the HIJING Model, used for event simulation, is also given.

3.1 Methodology

We studied the effects of the jet production on the following parameters; the multiplicity (N_{ch}), pseudorapidity (η), transverse momentum (p_T) and transverse mass (m_T) distributions of secondary charged particles produced in pp-interactions at 1.8 TeV in centre-of-mass system (CMS) frame as a function of different number of jets N_{jet}. We used the Dubna version of HIJING code, modified by V. V. Uzhinsky [109, 110], for simulation of 100,000 (one hundred thousands) events. These distributions for secondary charged (N_{ch}) particles, including protons, charged π ($\pi^{\pm}$) and charged K – mesons ($K^{\pm}$-meson) were considered. These distributions were considered for different number of jets (N_{jet}) and for the whole range and for different regions of the polar angle. The Number of jets was N_{jet}= D i.e. default values of jets, 0, 1 and 2, and labeled as D, 0, 1 and 2 respectively, as shown in Table 3.1. In the HIJING Model, the parameter for number of jets has default values D which represents the maximum number of jet production; it can be turned off i.e. 0 jets and can be fixed to any number 1, 2, and so on. Different angular regions were selected for six ranges of angle theta θ (in degrees): R1 (i.e. Region 1): θ=0°-2°, R2: θ=2°-4°, R3: θ=4°-6°, R4: θ=6°-10°, R5: θ=10°-30° and R6: θ=30°-90°. The reason for selection of these angular intervals R1-R6 was the statistical reliability of the data. We chose this selection of the polar angle regions from analyses of the angular distributions of the secondary charged particles.

Table 3.1 Values used for HIJING parameter for number of jet production, IHPR2(8) which can turned off and can set to any value IHPR2(8)<0 for its absolute values |IHPR2(8)|.

Values of HIJING parameter IHPR2(8)	Number of Jets (N_{jet})
D=10 (Default Value)	Maximum number of jets
0	0
-1	1
-2	2

As a first step we analyzed the multiplicity distributions of the charged particles produced in pp-collisions at 1.8 TeV as a function of N_{jet}=D, 0, 1 and 2, for full phase space (whole range of the polar angle) and for selected six regions R1—R6 of polar angle. Then we compared our analysis of the multiplicity distributions of charged particles with the analysis by the two component method of the superposition of the two negative binomial (NB) (Pascal) distributions for the experimental multiplicity distributions of charged particles in ppbar-collisions at 900 GeV by UA5 collaboration and at 1.8 TeV by Tevatron [111].

Then in continuation and confirmation of the HIJING code results on the influence of the jets on charged particles multiplicities (N_{ch}) in *pp*-collisions at 1.8 TeV, we carried out a detailed analysis of the pseudorapidity (η), transverse momentum (p_T) and transverse mass (m_T) distributions of secondary charged particles produced in *pp*-collisions at 1.8 TeV CMS energy as a function of N_{jet} for the whole range and selected six regions R1—R6 of the polar angle. Concerning the jet dependence of the pseudorapidity of the charged particles we made a qualitative comparison of the HIJING results for the pseudorapidity with the pseudorapidity spectra of the charged particles from the central detector at Fermilab (CDF) collaboration.

The relation that defines the pseudorapidity η is given by equation (2.7) in chapter 2 section 2.6.

Or in terms of the momentum $\vec{p}$, the pseudorapidity η can also be written as

$$\eta = \tfrac{1}{2}\ln\left(\frac{|\vec{p}| + p_L}{|\vec{p}| - p_L}\right) \tag{3.1}$$

where p_L is the component of the momentum along the beam direction (longitudinal momentum). In the high energy limit where the particle is travelling close to the speed of light, or in the approximation that the mass of the particle is nearly zero, numerically pseudorapidity η is equal to the rapidity y that is defined by the equation (2.6) in chapter 2 section 2.6.

The transverse momentum is defined by the equation (2.4) in chapter 2 section 2.6, and can also be written as:

$$p_T = p\sin\theta \tag{3.2}$$

The total momentum is given by:

$$p^2 = p_x^2 + p_y^2 + p_z^2 \tag{3.3}$$

with p_z the longitudinal momentum parallel to the beam (z-) axis.

The transverse mass is defined by the relation:

$$m_T = \sqrt{m^2 + p_T^2} \tag{3.4}$$

3.2 The HIJING Model

The heavy ion jet interaction generator (HIJING), a QCD inspired, Monte Carlo model, written in FORTRAN 77, was developed by M. Gyulassy and Xin-Nian Wang with special emphasis on the role of multiple mini-jets and multi-particle production in hadron-hadron (*pp*), hadron-nucleus (*pA*) and nucleus-nucleus (*AA*) interactions at collider energies. There are some special parameters in HIJING, like energy, frame (LAB: for fixed target experiment or centre of mass system (CMS): for colliding beam experiment), types of the colliding hadrons or nuclei, their impact parameter and some other parameters regarding the production of jets and other multi-particles, which users have to specify or change. Particularly, HIJING can reproduce many inclusive spectrum, two particle correlations, and can also explain the dependence of the average p_T on the multiplicity [112—114].

Our choice to use the HIJING model for the analysis is based on the fact that this model is specially designed for the study of multi-particle and multi-jet production in all kind of high energy interactions like *pp*, *pA* and *AA* which is one of the main advantages of this model over the others which are limited to only some particular hadronic interactions.

The concept of jet production and association of the jets with hard parton scattering is established very well for the hadronic collisions and these jets play an important role in many aspects of the $pp/p\bar{p}$ interactions at high energies. At hadron-hadron level of interaction, HIJING play an important role to deal with the interplay between low transverse momentum (p_T) non-perturbative physics and the hard perturbative quantum chromodynamics (pQCD) process. HIJING model has been extensively tested for the *pp* interactions data for a large range of collision energy [112—114].

In experiments, jets are being identified as showers of the hadrons whose transverse energy E_T could be reconstructed from the events' calorimetry [115, 116]. However, for the smaller transverse energy $E_T \langle 5GeV$ of a jet, it cannot be easily resolved from the underlying background [117], although it could be expected theoretically that the hard parton scatterings should continue for lower p_T. Usually these are referred to as minijets having too low transverse energy that cannot be experimentally resolved though the related parton scattering process could be calculated in the pQCD framework. Assuming independent production, the importance of the multiple minijets production in $p\bar{p}$ interactions has been shown to account for the increased total cross section [118].

The HIJING model contains some main subroutines, data blocks and event options and parameters. It contains the following two subroutines being called by users in the program [110, 113].

The first one is the HIJSET subroutine which initializes the HIJING and must be called prior to any other subroutine. In this subroutine the colliding energy and the frame (in fixed target experiment i.e. LAB or in the collider experiment, centre-of-mass system CMS) of the collisions is specified. This also specifies the nature of the projectile and the target whether these are hadrons (protons, neutrons, kaons, pions and their antiparticles) or the nuclei along with their charge and mass numbers.

The second one is the HIJING subroutine which can be repeatedly called after the HIJSET being called one time. This specifies the collisions frame i.e. the LAB or the CMS frame, and minimum and maximum values of the impact parameter which are randomly but evenly selected for hadron-nucleus and nucleus-nucleus collisions. For the case of pp collisions the events are averaged over all impact parameters.

Details about the main data blocks an event options and parameters of the HIJING model can be found in References [110, 113].

Chapter 4 Results and Discussions

The results obtained for different parameters of charged particles produced in *pp*-collisions at 1.8 TeV centre of mass energy using HIJING Model are presented and discussed in this chapter. The HIJING results for multiplicity and pseudorapidity distributions of charged particles are discussed in comparison with some available experimental results from SPS and Tevatron. The analysis presented here is based on the two papers in References [119, 120].

In order to study jet production or jet suppression and its effects on the different parameters of the charged particles produced in high energy collisions, it is useful to know the jet dependence of parameters like charged particles multiplicity, pseudorapidity and transverse momentum etc. in *pp*-collisions. Here we present an investigation of the jet dependence of the multiplicity, pseudorapidity, transverse momentum and transverse mass distributions of charged particles produced in *pp*-interactions at 1.8 TeV centre-of-mass energy using HIJING Monte Carlo model.

First we present the analysis of the charged multiplicity distributions as a function of N_{jet}=D, 0, 1 and 2, for whole range and selected six regions R1—R6 of the polar angle [119] and its comparison with analysis of SPS and Tevatron results by two component method [111]. The plots which show any spectra for N_{jet}=D, 0, 1 and 2 are obtained from the model and are not the experimental results.

4.1 The Multiplicity Distributions

Suppression of the jets [63, 64] in the high energy hadronic collisions is one of the clean signals on formation of the new states of strongly interacting matter, the quark gluon plasma (QGP), produced at extreme condition of high temperature and high baryon density. The jet quenching occurs due to the energy loss of jets at parton level [121]. To extract some information about this effect, the nuclear modification factor (NMF) is usually used as a function of the transverse momentum p_T [88, 122, 123]. The NMF is defined as

$$R_{AA}(p_T) \quad \frac{1}{\langle N_{coll}\rangle_C} \times \frac{d^2 N_{AA}^C / dp_T dy}{d^2 N_{pp} / dp_T dy} \tag{4.1}$$

where $d^2N^c_{AA}/dp_Tdy$ and d^2N_{pp}/dp_Tdy are the differential cross sections of secondary charged particles produced in central nucleus-nucleus and pp-interactions respectively at the same energy. $<N_{coll}>_C$ is a number of participant nucleons in the central nucleus-nucleus events [66], which could be defined using the Glauber approximation [124]. To study the jet suppression effect in hot and dense matter it is necessary to get full information on the jet production in *pp*-interactions. It is of great importance to understand how jet production can change the characteristics of the secondary particles produced in *pp*-collisions. Apparently it is not simple question to get complete information on the jet production in *pp*-collisions at any energy. It will be very interesting to analyze the jet production in conditions of 4π geometry measurements to see full picture of the interactions.

Modern simulation packages give possibilities to analyze the interactions under necessary conditions of 4π geometry measurements. In this section we present the study of the jet production in ultrarelativistic pp-collisions using heavy ion jet interaction generator (HIJING) Monte Carlo model [112—114].

In paper, by Roberto Ugoccioni and Alberto Giovannini [111], the multiplicity distribution (MD) of the secondary charged particles produced in the $p\bar{p}$ collisions at 900 GeV from UA5 collaboration [125, 126] is described by the weighted superposition of two negative binomial (NB) (Pascal) multiplicity distribution (see Figure 4.1).

The negative binomial Pascal multiplicity distribution for two-parameters can be expressed as:

$$P_n^{(Pascal)}(\bar{n}, k) \quad \frac{k(k+1)\cdot\dots\cdot(k+n-1)}{n!} \frac{\bar{n}^n k^k}{(\bar{n}+k)^{n+k}} \tag{4.2}$$

Where $\bar{n}$ is the average value of the multiplicity and $\frac{1}{k}$ is the measure of the deviation of the variance $D^2 \;\; \langle n^2 \rangle - \bar{n}^2$ from Poisson shape $\frac{1}{k} + \frac{1}{\bar{n}} \;\; \frac{D^2}{\bar{n}^2}$. Actually for the case of Poisson distribution where $k \to \infty$, $D^2 \;\; \bar{n}$ and in case of geometric distribution where $k \;\; 1$, $D^2 \;\; \bar{n} + \bar{n}^2$.

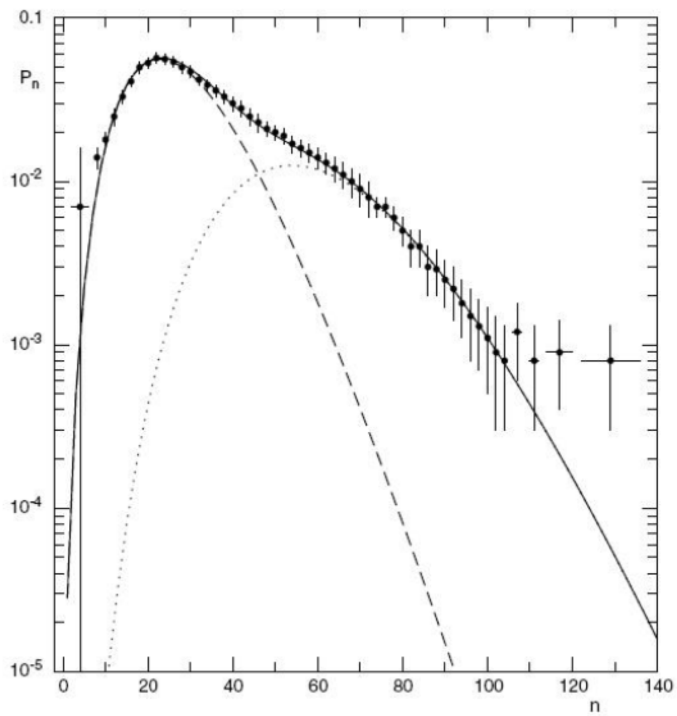

Figure 4.1 Multiplicity distribution for charged particles produced in the $p\bar{p}$ reaction at 900 GeV obtained by the UA5 collaboration. The lines are the result of fitting [111].

The distribution shows two regions in the behavior of the multiplicity distribution: 10<n<60 and 60<n<120; semi hard and soft events. The multiplicity distribution of each class can be described well by the Pascal distribution, which itself could not reproduce the shoulder structure appeared in the UA5 results at 900 GeV. For Fermilab results they found for E735 data (Figure 4.2) that the soft component satisfies the Koba-Nielsen-Olesen (KNO) scaling [127, 128] and hard one does not.

According to the Polyakov and Koba-Nielsen-Olesen hypothesis, at extremely high energy s the probability $P_n(s)$ of n particles production in a particular interaction must exhibit the following relation:

$$P_n(s) = \frac{1}{\langle n(s) \rangle} \psi(z) \tag{4.3}$$

where $z = \frac{n}{\langle n(s) \rangle}$ is the scaled multiplicity with $\langle n(s) \rangle$ as average values of the secondary particles multiplicity at the colliding energy s. According to this scaling hypothesis if $P_n(s)$ for different values of s is rescaled by stretching the horizontal or vertical axis with average values $\langle n(s) \rangle$ then the rescaled distributions will coincide. Which means that the multiplicity distributions get simply rescaled copies of the universal scaling function $\psi(z)$, and depend only on the $z = \frac{n}{\langle n(s) \rangle}$ [127, 128].

They concluded that the weighted superposition mechanism of two negative binomial (Pascal) distributions describe well the multiplicity distributions in pp collisions. In hadronic collisions, the two components correspond to soft events and to semi-hard events respectively. Based on this mechanism, the knowledge of the features of multiplicity distributions up to 900 GeV centre of mass energy has been used to predict the characteristic behavior expected in the TeV energy range: the soft component satisfies KNO scaling, while the semi-hard one violates it strongly [111].

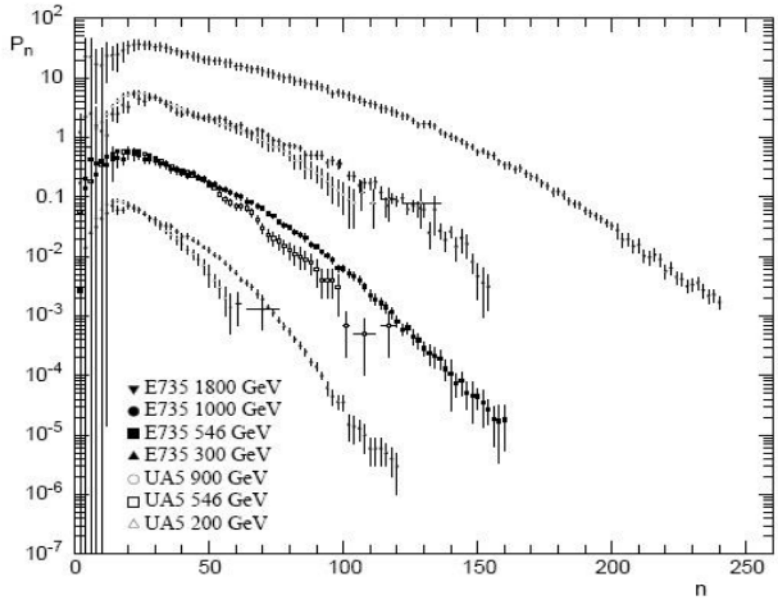

Figure 4.2 Multiplicity distribution of secondary charged particles in the $p\bar{p}$ reactions at Tevatron energies obtained by the E735 [111, 129, 130].

4.2 Simulation Results for N_{ch} in *pp*-Interactions at 1.8 TeV

We have analyzed multiplicity distributions of the secondary charged particles produced in *pp*-collision at 1.8 TeV centre of mass system (CMS) energy. Dubna version of HIJING code (modified by V. V. Uzhinsky [109, 110]) is used for 100,000 (one hundred thousands) events. The multiplicity distribution of secondary charged (N_{ch}) particles, including protons, charged π ($\pi^{\pm}$) and charged K – mesons ($K^{\pm}$-meson) is considered. The N_{ch}-distributions were considered for different number of jets (N_{jet}) and for different locations of jets i.e. different polar angle ranges. Number of jets was $N_{jet}= D$ i.e. default values of jets, 0, 1 and 2 (and labeled as D, 0, 1 and 2 respectively). Different angular regions were selected for six ranges of angle theta θ (in degree): 0-2 (R1 i.e. region 1), 2-4 (R2), 4-6 (R3), 6-10 (R4), 10-30 (R5) and 30-90 (R6).

Figure 4.3 shows the multiplicity distribution of secondary charged particles produced in *pp* interaction at 1.8 TeV. The model gives three regions in contrast to the experiment having two regions only (see Figure 4.1). It is connected with elastic scattering and diffractive events in the model that result in the leading particle effect [131-135]. The first region corresponds to the values of multiplicity for $N_{ch}< 15$; second one is for $15 < N_{ch} <80$ and third for $N_{ch}>80$. Figure 4.3 shows that the first region is formed mainly due to the events with 0 jet (here we have sharp peak), second one is contributed by multi-jet events along with zero jet events and third region is contributed only due to multi-jet events. So the analyses demonstrate that jet production can change the behavior of N_{ch}-distribution in various regions of multiplicity differently. The model data demonstrate that multijet cases will influence essentially in high multiplicity area ($N_{ch}>120$). As we have mentioned above that second and the third regions were described by the weighted superposition of two negative binomial (NB) (Pascal) multiplicity distribution [111].

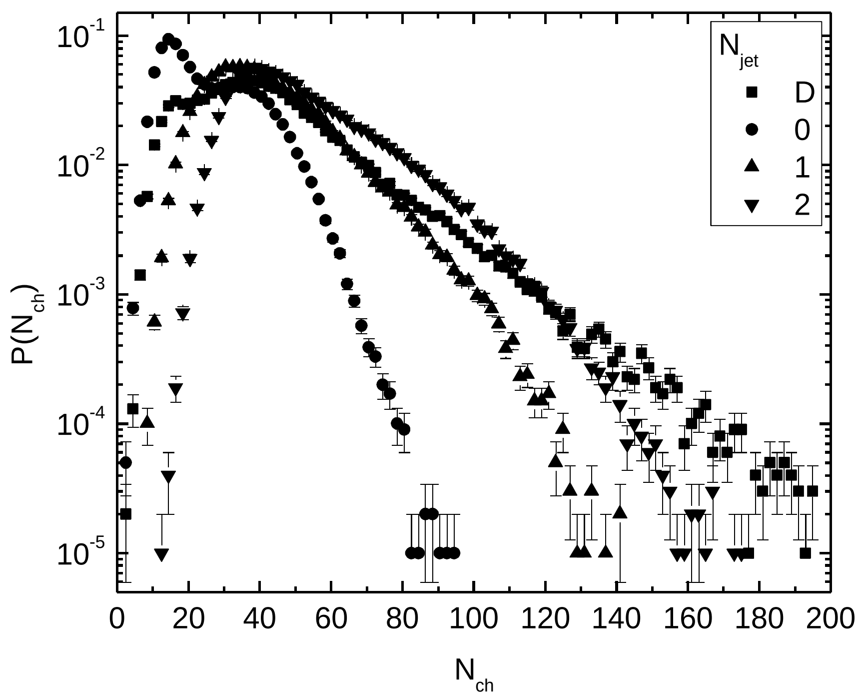

Figure 4.3 The multiplicity distribution of N_{ch} for N_{jet}= D, 0, 1 and 2 for whole range of polar angle.

Now let us consider that how the jet production will influence the angular distributions of particles. Figures 4.4—4.9 demonstrate the N_{ch}—distributions for charged particles produced in pp-interaction at $\sqrt{s}$=1.8 TeV. We have simulated 100,000 (one hundred thousands) events with N_{jet}=D, 0, 1 and 2, for different regions of angles from R1 to R6.

Figure 4.4 shows that jet production do not influence essentially the multiplicity distribution. The result can be explained in the following way. Since the first angular region $\theta = 0^o$-2^o - R1 mainly consists of particles with high longitudinal momentum but the jets are high p_T particles. This figure also indicates that the first peak in the Figure 4.3 is mainly due to the events with N_{jet}=0.

The Figures 4.5—4.9 (R2—R6) show that with increasing the polar angle of the particles the jet production changes essentially the multiplicity spectrum of the particles (as observed in Figure 4.3) in the regions $15 < N_{ch} < 80$ and $N_{ch} > 80$.

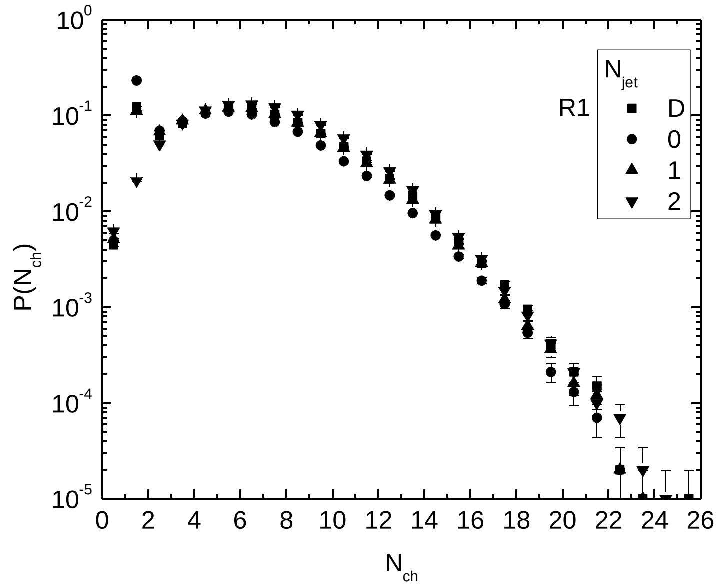

Figure 4.4 The multiplicity distribution of charged particles for N_{jet}= D, 0, 1 and 2 in angular region R1 0-2 degree.

The Figure 4.5 for angular region R2 θ=2-4° shows that jets influence the multiplicity in this region. Increasing the polar angle thus increases the p_T of particles contributing jets. It can also be seen that multiplicity is affected (increased) by 1, 2 and default jet events as compared to 0 jet events. This increasing effect in multiplicity can also be seen for next angular region R3 θ=4-6° shown in Figure 4.6. But here 2 and default jet events has more increasing effect on multiplicity as compared to the 1 and 0 jet events. Figure 4.7 for angular region R4 θ=6-10° shows a similar behavior as was observed in Figure 4.6 but with a more increase in multiplicity. This trend continued in the last two angular regions: Figure 4.8 for R5 θ=10-30° and Figure 4.9 for R6 θ=30-90°. Since these are also large p_T particles regions, therefore by increasing the polar angle the multiplicity with increasing number of jets is much more increased as compared to other regions. These angular regions also show that these have more contribution to change (increase) the multiplicity as is also evident in last two regions of Figure 4.3.

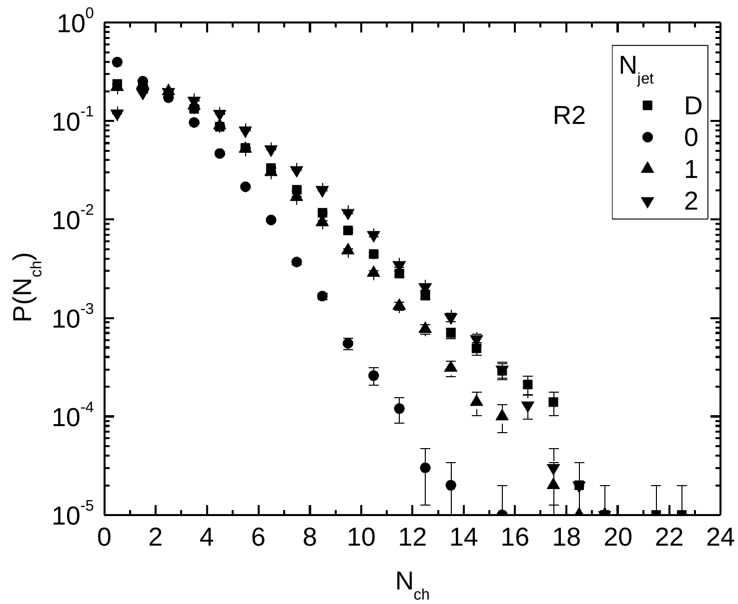

Figure 4.5 The multiplicity distribution of charged particles for N_{jet}=D, 0, 1 and 2 in angular region R2 2-4 degree.

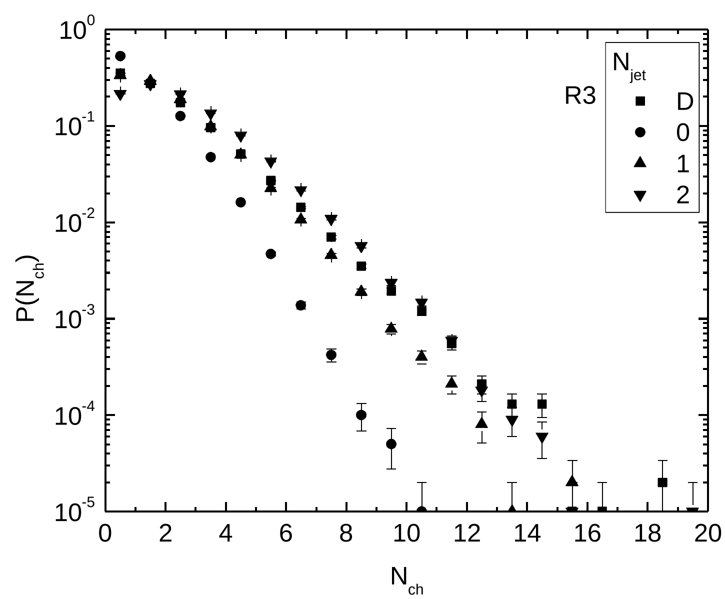

Figure 4.6 The multiplicity distribution of charged particles for N_{jet}= D, 0, 1 and 2 in angular region R3 4-6 degree.

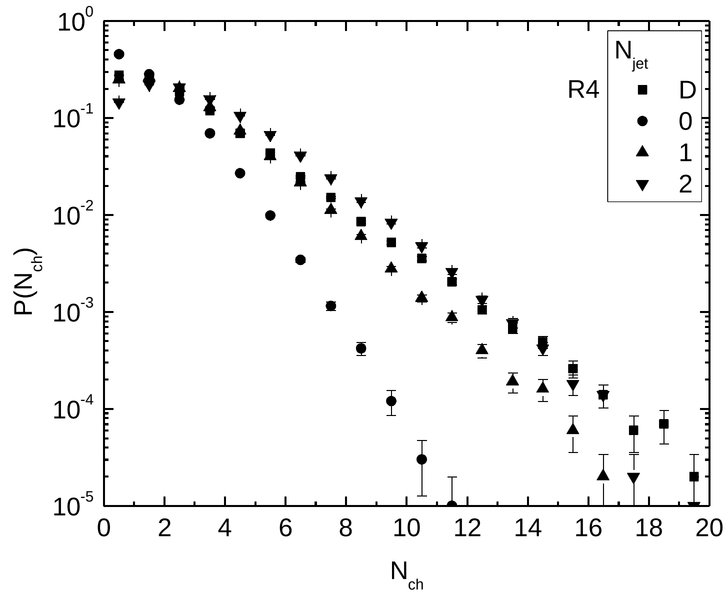

Figure 4.7 The multiplicity distribution of charged particles for N_{jet}= D, 0, 1 and 2 in angular region R4 6-10 degree.

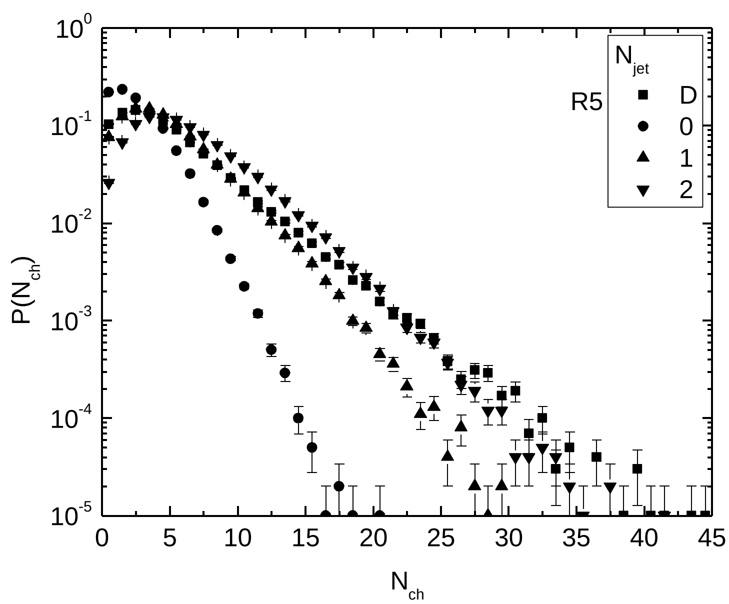

Figure 4.8 The multiplicity distribution of N_{ch} for N_{jet}= D, 0, 1 and 2 in angular region R5 10-30 degree.

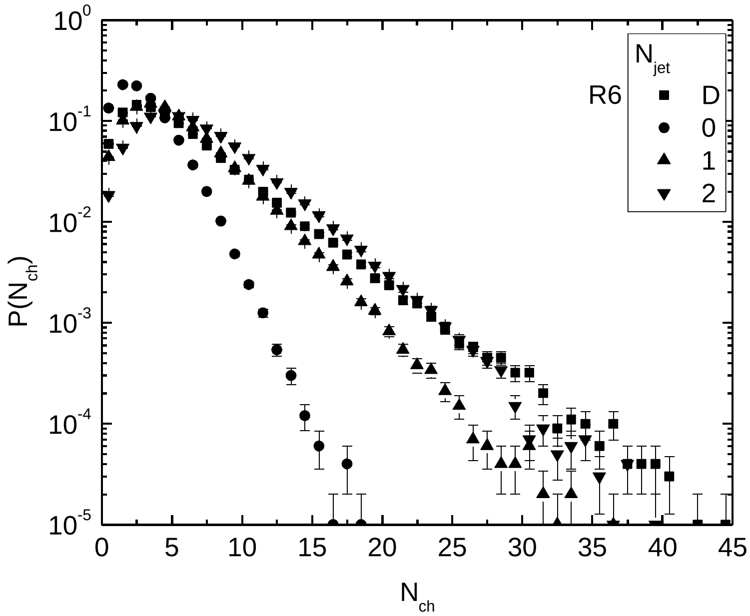

Figure 4.9 The multiplicity distribution of charged particles for N_{jet}= D, 0, 1 and 2 in angular region R6 30-90 degree.

For this section we conclude that the simulation data coming from the HIJING code show that there are three areas in multiplicity distributions of secondary charged particles: $N_{ch}<15$, $15 < N_{ch}<80$ and $N_{ch}>80$. We identified the first area as a region dominating leading particles: elastic scattering region. The particles from this area correspond to the polar angle region 0-2 degree and without jets. The second region corresponds mainly to multi-jet events along with contribution from the zero jet events. The third area corresponds mainly to multi-jet (1, 2 or more jets) events. Analysis of the multiplicity distributions for other angular regions (2-90 degrees) also showed that the increase in the charged particles multiplicity is connected to the multi-jet events in the *pp* collisions at TeV energy scale. So we could conclude that for the HIJING simulation results for pp collisions at TeV energy scale, in the multiplicity distributions for full polar angle range first area corresponds mainly to leading particles, second area corresponds mainly to multi-jet events along with zero jet events and third area corresponds mainly to multi-jet events as these areas has a similar description in the weighted superposition mechanism of two negative binomial multiplicity distributions for hadronic collisions where the two components correspond to soft and semi-hard events respectively.

4.3 Simulation Results for η, p_T and m_T in *pp* Interactions at 1.8 TeV

Now in the following three sections we present the study which is a continuation and confirmation of the HIJING code results, presented above, on the influence of the jets on charged particles multiplicities (N_{ch}) in *pp*-collisions at 1.8 TeV [119], where we presented and discussed the increase observed in N_{ch} as a function of different number of jets for charged particles distributions in full phase space (whole polar angle rage) and for six different regions of the polar angle θ (R1: θ=0-2°, R2: θ=2-4°, R3: θ=4-6°, R4: θ=6-10°, R5: θ=10-30° and R6: θ=30-90°). The results of distributions of N_{ch} for zero and multi-jet events were found to be inconsistent with the experimental multiplicity distributions (MDs) of charged particles interpreted by fitting with the Pascal (negative binomial) distributions [111].

Lets discuss the results for the effects of jet production on pseudorapidity (η), transverse momentum (p_T) and transverse mass (m_T) distributions of secondary charged particles as a function of N_{jet}=D, 0, 1 and 2 for the whole polar angle range and also for six selected regions of polar angle R1 to R6 [120]. The parameters pseudorapidity η and transverse momentum p_T are defined by equations (2.7) and (2.4) respectively in chapter 2, section 2.6, and transverse mass m_T is defined by the equation (3.4) in chapter 3 section 3.1. Here, we have studied the results for η-, p_T- and m_T-distributions of secondary charged particles for the whole polar angle range and for six regions in comparison with the reported results for change (increase) in multiplicity of N_{ch} in multi-jet events [119]. Moreover, these results are discussed in connection with the experimental results for pseudorapidity distributions of charged particles from the Collider Detector at Fermilab (CDF Collaboration) [136].

We have analyzed η-, p_T- and m_T -distributions of the secondary charged particles produced in *pp*-collisions at 1.8 TeV centre of mass energy. The Dubna version of the HIJING code (modified by Uzhinsky [109, 110]) is used for simulation of 100,000 events. These distributions of secondary charged particles, including protons, charged π ($\pi^{\pm}$) and charged K – mesons ($K^{\pm}$-meson) are considered. These distributions are considered for different numbers of jets (N_{jet}) for the whole range of the polar angle as well as in its different regions. The number of jets was N_{jet}= D, i.e. the default value of jets (maximum number) taken from the HIJING model, 0, 1 and 2 (and labeled as D, 0, 1 and 2 respectively). Different angular regions were selected for six ranges of the polar angle theta θ (in degrees) from R1 to R6.

4.4 The Pseudorapidity Distributions

The pseudorapidity distribution of charged particles (for example in the range $0 < \eta < 8$) produced in *pp*-collisions at 1.8 TeV, as a function of number of jets N_{jet}=D, 0, 1 and 2, is shown in Figure 4.10. This figure shows some plateaus for the central pseudorapidity regions (in the area about $0 < \eta < 4$).

The existence of plateaus in rapidity or pseudorapidity is very important for theoretical estimation. For example, J. D. Bjorken described the space-time evolution of the hadronic matter produced in the central rapidity region in extreme nucleus-nucleus collisions [137]. He found that quark-gluon plasma is produced at a temperature of the order of 200 MeV, which was in agreement with previous measurements [138]. The author also commented that the description relies on the existence of a flat central plateau and on the applicability of hydrodynamics.

Here in Figure 4.10, one can see that with increasing number of jets:

- the width of the distribution/plateaus is decreased,
- the pseudorapidity density in the central area is increased.

- the pseudorapidity spectrum for N_{jet}=2 events are systematically higher than that of N_{jet}=0 events, which shows that 2 (multi)-jet events lead to an increase in the pseudorapidity density.

The existence of the plateaus in the rapidity/pseudorapidity distributions is also important for the applicability of hydrodynamics. According to the Bjorken model [137], usually used to estimate the QGP parameters, the density of energy (transverse flow neglected) is given by the relation

$$\varepsilon_{BJ} \quad \frac{Energy}{Volume} \quad \frac{\frac{dE_T}{d\eta}}{\pi R_0^2 A^{2/3} c\tau_0} \quad \frac{m_T \frac{dN}{d\eta}}{\pi R_0^2 A^{2/3} c\tau_0} \tag{4.4}$$

where $\pi R_0^2 A^{2/3}$ is the transverse size of the smallest nucleus; $\tau_o \sim 1\ fm/c$ is formation time and $\frac{dE_T}{d\eta} \quad m_T \frac{dN}{d\eta}$ is mean energy of the particle, multiplied by the number of particles; $m_T \quad \sqrt{m^2 + p_T^2}$ is transverse mass (or energy) . In this model if the mean free path is ~ 0.5 *fm* then $\varepsilon_{BJ} \sim 2\ GeV/fm^3$.

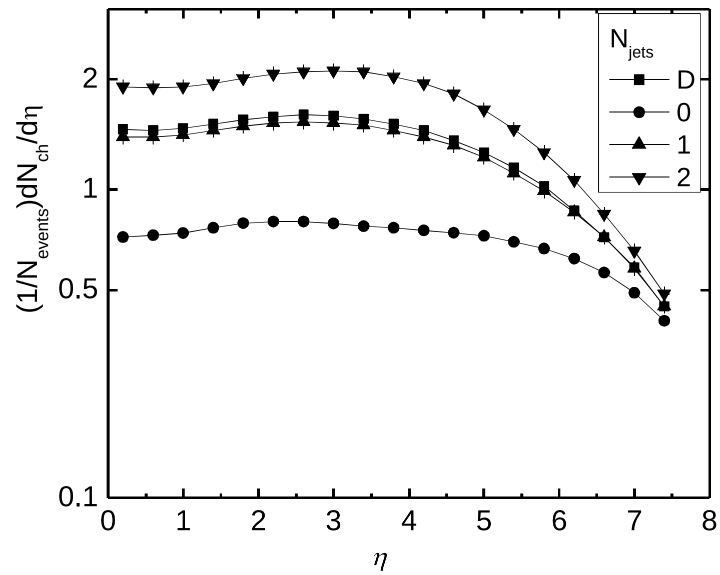

Figure 4.10 The η-distributions of charged particles produced in *pp* collisions at 1.8 TeV for N_{jet}=D, 0, 1 and 2.

In Figure 4.11 the data are presented for the corrected η distributions (corrected for geometric and kinematic acceptance, tracking efficiency etc.) of charged particles produced in proton-antiproton collisions at $\sqrt{s}$=1800 and 630 GeV from the collider detector at Fermilab [136]. A measurement from the CERN SPS collider performed by UA5 at $\sqrt{s}$=546 GeV is also shown in this figure. A qualitative comparison of these data with those from Figure 4.10 for the pseudorapidity region $|\eta|\leq 3.5$ demonstrates that as the η spectra for CDF Tevatron data are much higher than those for the HIJING (N_{jet}=2) data, this increase in pseudorapidity density is due to multi-jet events.

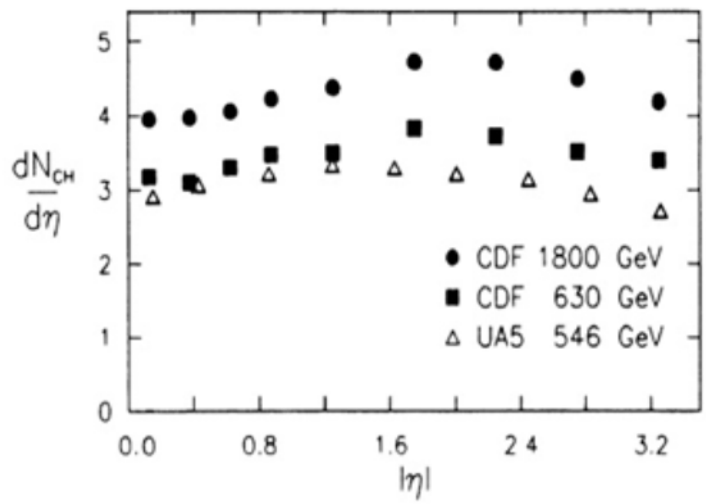

Figure 4.11 The pseudorapidity density measured by the CDF collaboration at 1800 and 630 GeV, and by the UA5 collaboration at 546 GeV [136].

As the polar angle for zero to 90 degrees correspond to the pseudorapidity region ~8 to zero, so the pseudorapidity spectra for six regions of polar angle R1 to R6 are also included in Figure 4.10.

4.5 The Transverse Momentum Distributions

In Figure 4.12 and Figures 4.13 to 4.18 the transverse momentum p_T distributions of secondary charged particles produced in *pp*-interactions at 1.8 TeV as a function of number of jets N_{jet}=D, 0, 1 and 2, are presented, for the whole range and for the six selected regions (R1 to R6) of the polar angle. We can see that with increasing the number of jets from 0 to 1, 2 or with the default values of jets the transverse momentum is increased as the jets or multi-jet events contain high p_T particles.

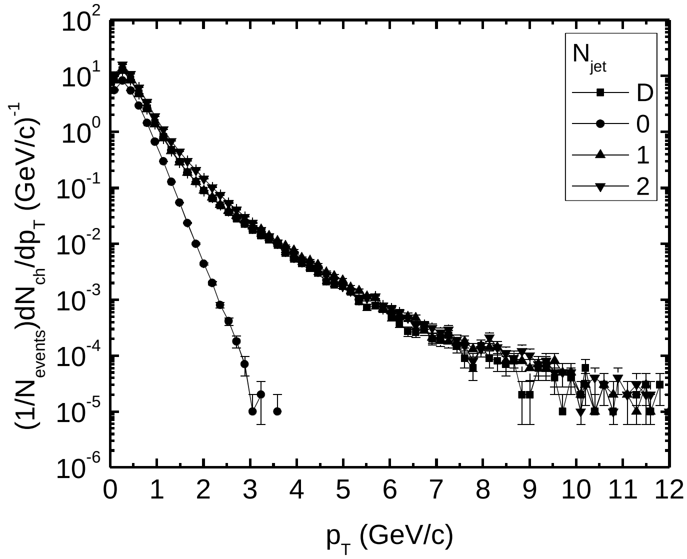

Figure 4.12 p_T distribution of charged particles for N_{jet}=D, 0, 1 and 2 for the whole range of polar angle.

The shape of the distributions in the case of $N_{jet} \geq 1$ is different in two areas of p_T: p_T<2 GeV/c and p_T>2 GeV/c. The slopes of the distributions in the first area are very close to that of the events with N_{jet}=0 (slopes of the p_T distributions for the whole θ-range and for regions R1-R6 are shown in Tables 4.1 and 4.2 and plotted in Figure 4.19). So we could say that particles with p_T<2 GeV/c are produced by the same dynamics in events with different N_{jet}, i.e. there is no jet dependence in the p_T<2 GeV/c region (or zero-jet events have no contribution to the p_T>2 GeV/c region). The particles with p_T>2 GeV/c are those produced by some special dynamics, different from the particles produced with p_T<2 GeV/c; namely, the jet dynamics (production and hadronization of the jets) from the HIJING code. In our previous study [119] we also observed two regions for the multiplicity distribution of charged particles. We concluded that the high multiplicity regions in the N_{ch}-distribution correspond to the multi-jet events. The results were in good agreement with those discussed by Ugoccioni and Giovannini [111].

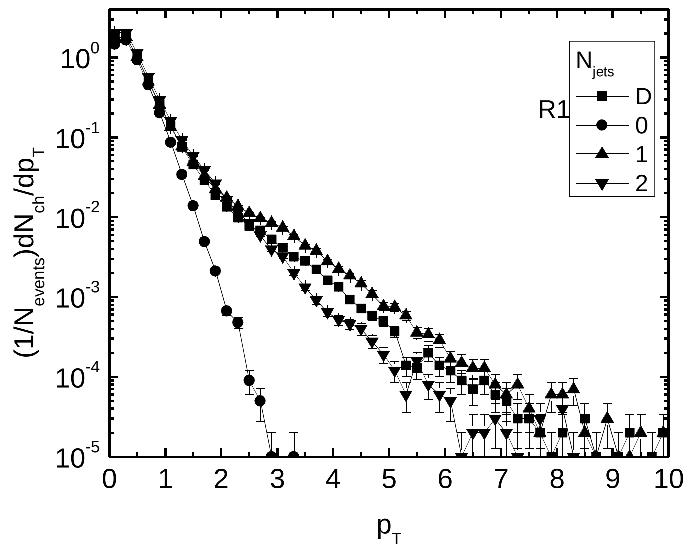

Figure 4.13 p_T distributions of charged particles for N_{jet}=D, 0, 1 and 2 in the angular region: R1 θ=0-2°.

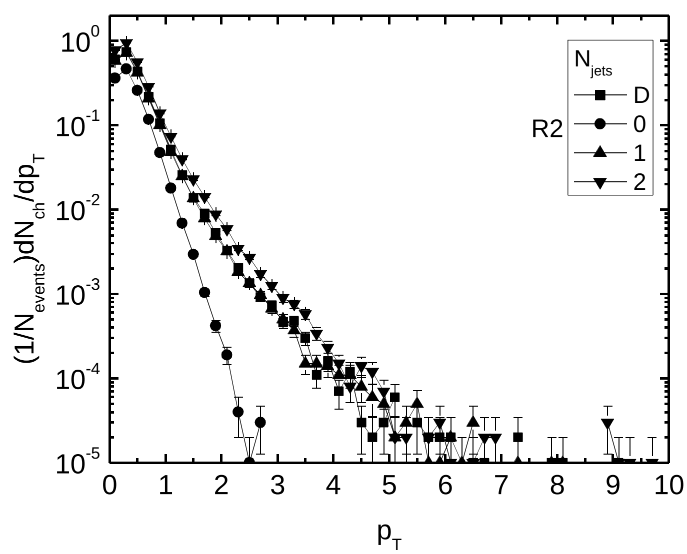

Figure 4.14 p_T distributions of charged particles for N_{jet}=D, 0, 1 and 2 in the angular region: R2 θ=2-4°.

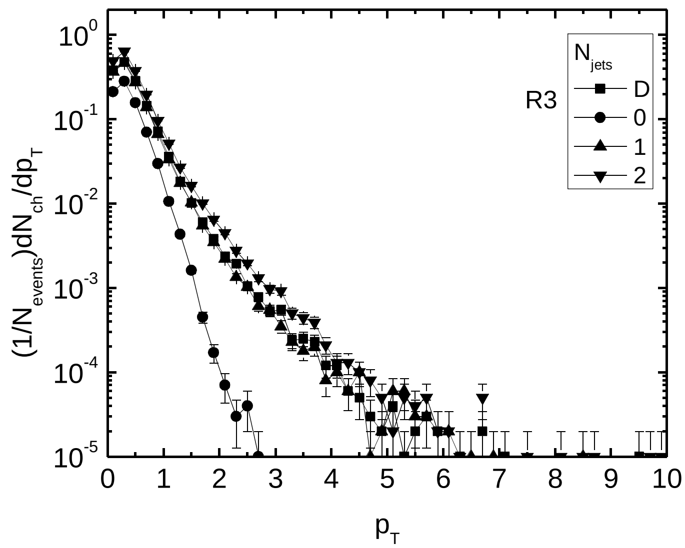

Figure 4.15 p_T distributions of charged particles for N_{jet}=D, 0, 1 and 2 in the angular region: R3 θ=4-6°.

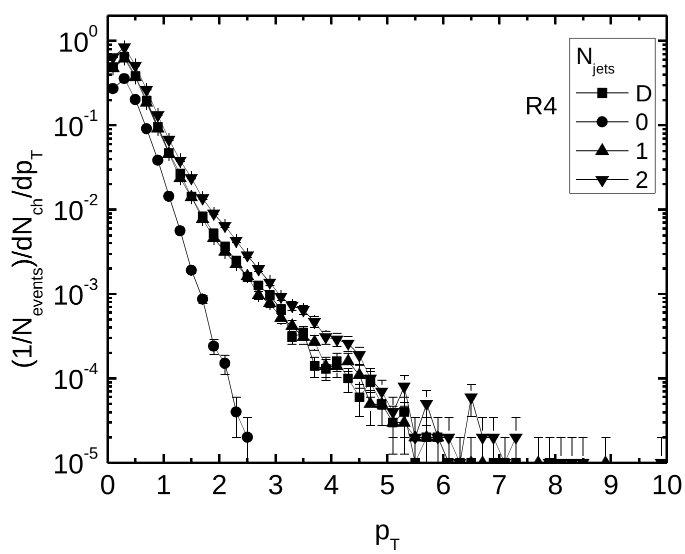

Figure 4.16 p_T distributions of charged particles for N_{jet}=D, 0, 1 and 2 in the angular region: R4 θ=6-10°.

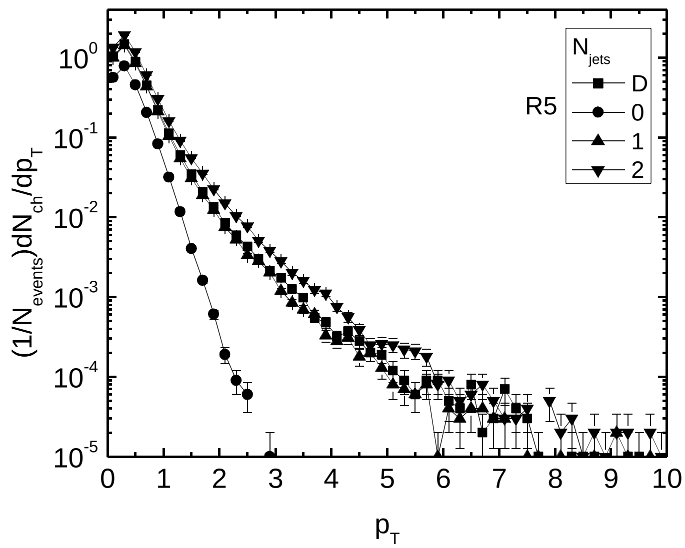

Figure 4.17 p_T distributions of charged particles for N_{jet}=D, 0, 1 and 2 in the angular region: R5 θ=10-30°.

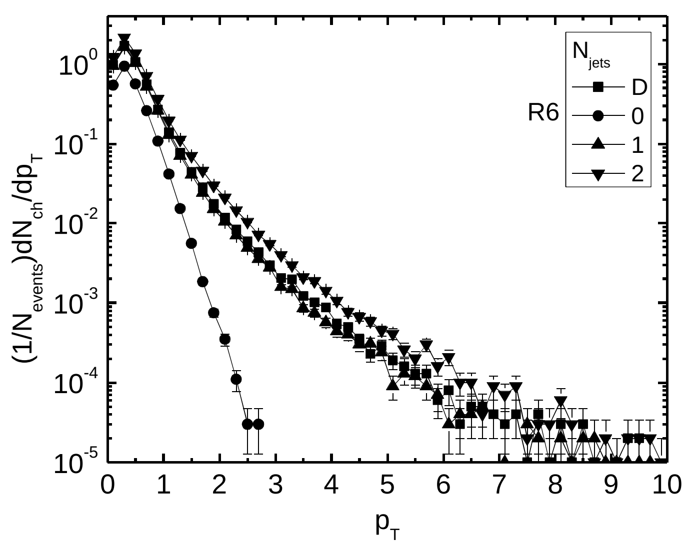

Figure 4.18 p_T distributions of charged particles for N_{jet}=D, 0, 1 and 2 in the angular region: R6 θ=30-90°.

Figures 4.13 to 4.18 demonstrate how the increase in values of the p_T spectra depends on the polar angle of the produced charged particles (as $p_T \quad p\sin\theta$). This shows the dependence of the variation in the p_T spectra with respect to the polar angle (the angular regions R1—R6) and its dependence on N_{jets}.

The slopes parameters obtained by using the exponentially decaying fit function e^{-bx} with b as the slope parameter, for transverse momentum distributions for the whole range and for selected six regions R1—R6 of polar angle in the p_T regions p_T<2GeV/c and 2GeV/c< p_T<3GeV/c are listed in Tables 4.1 and 4.2 respectively.

Table 4.1 Slopes of the p_T spectra for the whole range and selected regions R1—R6 of the polar angle for p_T<2GeV/c

Polar Angle θ	N_{jet}=D	N_{jet}=0	N_{jet}=1	N_{jet}=2
whole range	3.10±2.61E-4	3.80±2.72E-4	3.13±2.62E-4	3.03±2.48E-4
R1 θ=0°-2°	3.25±7.07E-4	3.61±5.33E-4	3.30±7.15E-4	3.23±6.88E-4
R2 θ=2°-4°	3.28±1.02E-3	3.80±9.25E-4	3.31±1.02E-3	3.19±9.64E-4
R3 θ=4°-6°	3.20±1.32E-3	3.81±1.16E-3	3.24±1.32E-3	3.15±1.21E-3
R4 θ=6°-10°	3.20±1.15E-3	3.81±1.06E-3	3.21±1.15E-3	3.11±1.06E-3
R5 θ=10°-30°	3.18±7.67E-4	3.80±6.9E-4	3.21±7.63E-4	3.07±7.22E-4
R6 θ=30°-90°	3.07±7.55E-4	3.71±6.55E-4	3.11±7.47E-4	3.08±7.23E-4

Table 4.2 Slopes of the p_T spectra for the whole range and selected regions R1—R6 of the polar angle for 2GeV/c<p_T<3GeV/c

Polar Angle θ	N_{jet}=D	N_{jet}=0	N_{jet}=1	N_{jet}=2
whole range	1.87±0.01	4.61±0.01	1.77±0.02	1.95±0.01
R1 θ=0°-2°	1.17±0.06	3.99±0.05	0.76±0.14	1.68±0.02
R2 θ=2°-4°	1.98±0.04	4.64±0.07	1.99±0.04	1.93±0.03
R3 θ=4°-6°	1.96±0.05	4.58±0.06	1.93±0.05	1.97±0.04
R4 θ=6°-10°	1.77±0.04	4.44±0.06	1.88±0.05	2.10±0.03
R5 θ=10°-30°	1.67±0.04	4.14±0.07	1.79±0.03	1.89±0.02
R6 θ=30°-90°	1.85±0.03	4.22±0.05	1.86±0.03	1.84±0.02

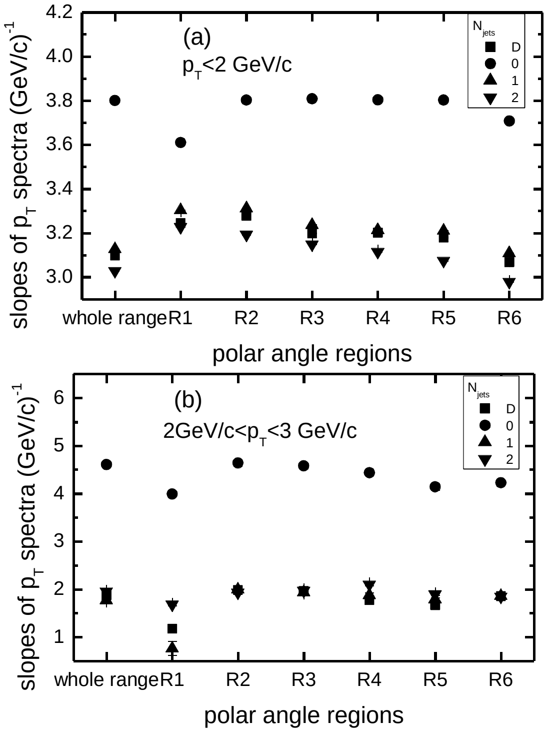

Figure 4.19 Slopes of the p_T spectra for the whole range and selected regions R1-R6 of the polar angle, *(a)* for p_T<2GeV/c and *(b)* for 2GeV/c<p_T<3GeV/c

In Figure 4.19 (*(a)* and *(b)*), plots are shown for the slopes of the p_T spectra for the whole range and selected six regions R1-R6 of the polar angle for p_T<2GeV/c and for 2GeV/c<p_T<3GeV/c as a function of N_{jets}. This supports the analysis described above for the p_T spectra.

4.6 The Transverse Mass Distributions

We now consider the transverse mass m_T distributions of secondary charged particles produced in *pp*-interactions at 1.8 TeV as a function of number of jets N_{jet}=D, 0, 1 and 2, for the whole range and the six selected regions (R1 to R6) of the polar angle. It is well known that the m_T distributions are more sensitive to the temperature of the systems. Figure 4.20 shows the m_T distributions of secondary charged particles produced in *pp*-interactions at 1.8 TeV for N_{jet}=D, 0, 1 and 2 for the whole polar angle range. With increasing the number of jets from 0 to 1, 2 or the default value of jets, an increase in the transverse mass is observed and here the increase in the case of multi-jet events is more than for the transverse momentum distributions as transverse mass is $m_T \quad \sqrt{m^2 + p_T^2}$.

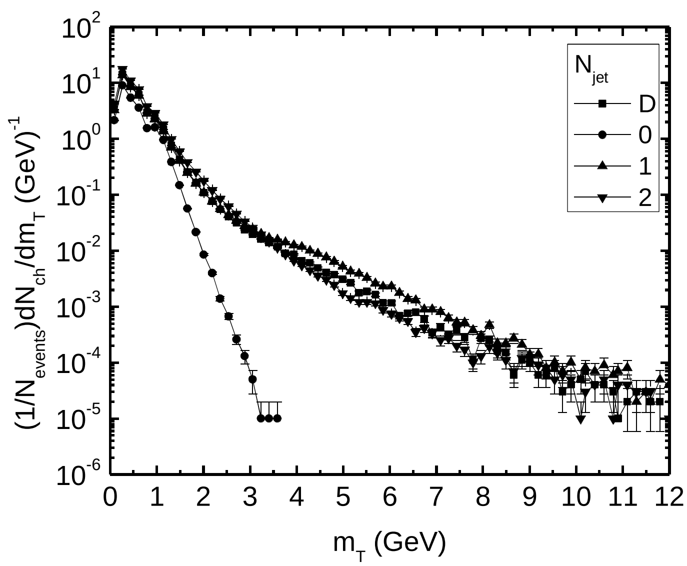

Figure 4.20 m_T distribution of charged particles for N_{jet}=D, 0, 1 and 2 for the whole range of polar angle.

Transverse mass distributions of secondary charged particles for *pp*-collisions at 1.8 TeV, for the six selected regions (R1—R6) of polar angle, are shown in Figures 4.21 to 4.26. An increase in m_T similar to that in p_T is observed in all regions except for the angular region R1 θ=0-2°, where multi-jet events have a higher increment for m_T which may be due to the elastic scattering events in *pp*-interactions. The region R1 may also be affected by the leading particle effect [131-135] with particles containing high longitudinal and low transverse momentum, as was observed in our previous study in the case of N_{ch} distribution for the same polar angle region and also in the low N_{ch} region for multiplicity distributions for full phase space [119]. We can see that the slopes of the distributions depend on the polar angle of the particles and the number of jets for the high p_T particles (p_T>2 GeV/c).

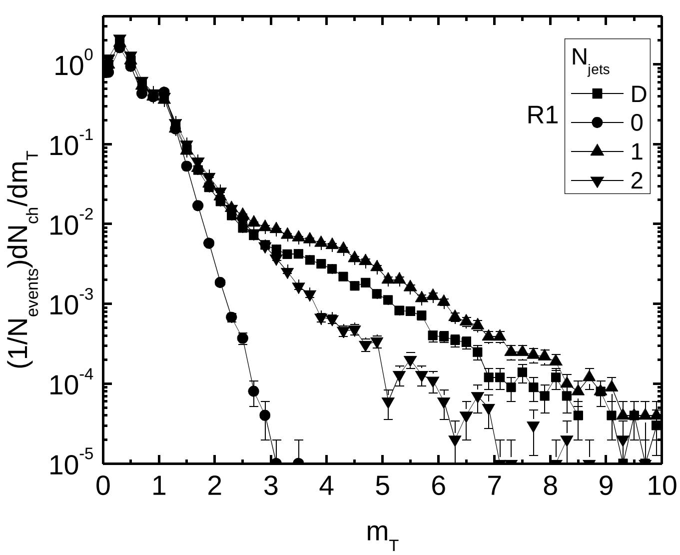

Figure 4.21 m_T distributions of charged particles for N_{jet}=D, 0, 1 and 2 in the angular region: R1 θ=0-2°.

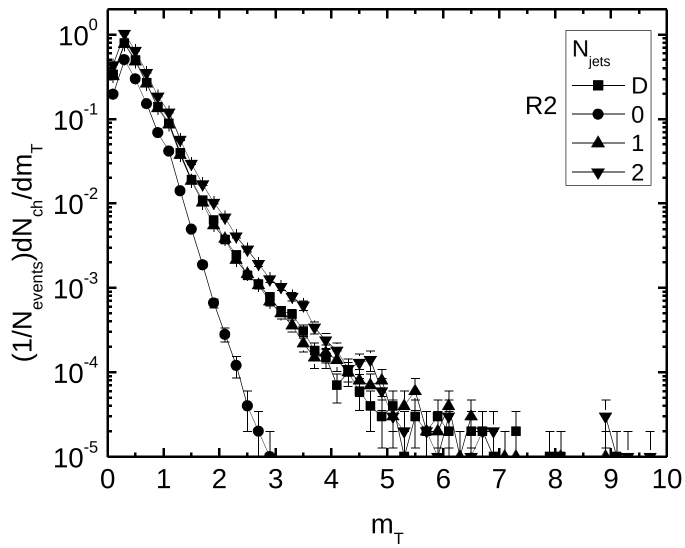

Figure 4.22 m_T distributions of charged particles for N_{jet}=D, 0, 1 and 2 in the angular region: R2 θ=2-4°.

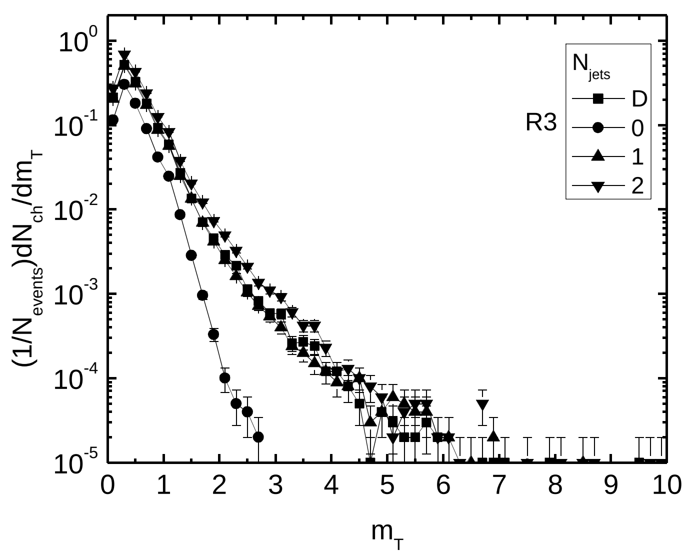

Figure 4.23 m_T distributions of charged particles for N_{jet}=D, 0, 1 and 2 in the angular region: R3 θ=4-6°.

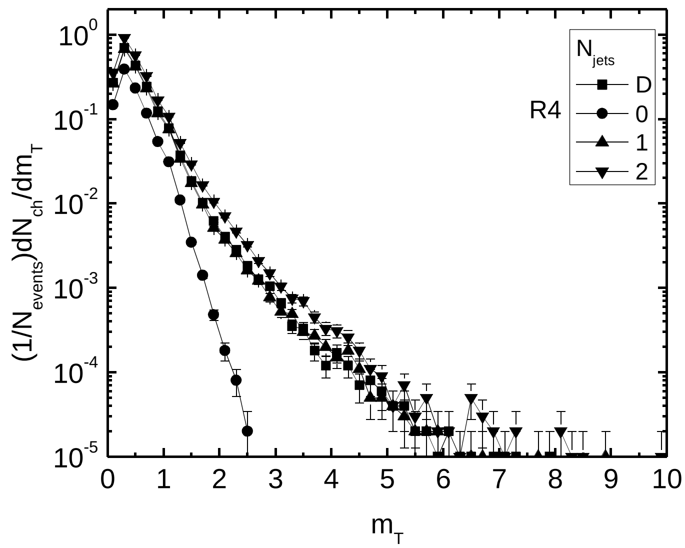

Figure 4.24 m_T distributions of charged particles for N_{jet}=D, 0, 1 and 2 in the angular region: R4 θ=6-10°.

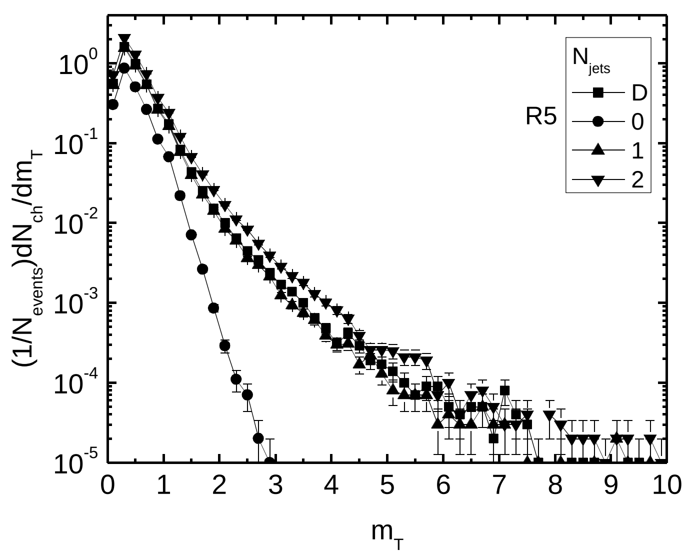

Figure 4.25 m_T distributions of charged particles for N_{jet}=D, 0, 1 and 2 in the angular region: R5 θ=10-30°.

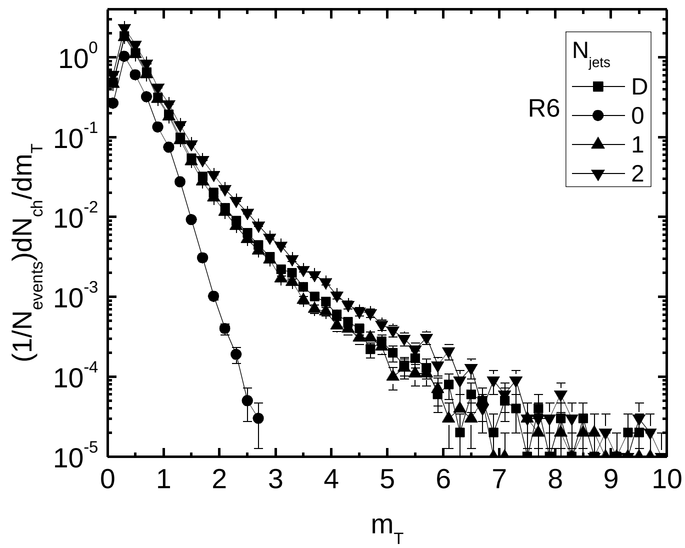

Figure 4.26 m_T distributions of charged particles for N_{jet}=D, 0, 1 and 2 in the angular region: R6 θ=30-90°.

Tables 4.3 and 4.4 show the slope parameters of transverse mass distributions for the whole range and for selected six regions R1—R6 of polar angle in the m_T regions m_T<2GeVand 2GeV< m_T<3GeV respectively. These slopes parameters are obtained by using the exponentially decaying fit function e^{-bx} with b as the slope parameter.

Table 4.3 Slopes of the m_T spectra for the whole range and selected regions R1-R6 of the polar angle for m_T<2GeV

Polar Angle θ	N_{jet}=D	N_{jet}=0	N_{jet}=1	N_{jet}=2
whole range	3.10±2.61E-4	3.80±2.72E-4	3.13±2.62E-4	3.03±2.48E-4
R1 θ=0°-2°	3.25±7.07E-4	3.61±5.33E-4	3.30±7.15E-4	3.23±6.88E-4
R2 θ=2°-4°	3.28±1.02E-3	3.80±9.25E-4	3.31±1.02E-3	3.19±9.64E-4
R3 θ=4°-6°	3.20±1.32E-3	3.81±1.16E-3	3.24±1.32E-3	3.15±1.21E-3
R4 θ=6°-10°	3.20±1.15E-3	3.81±1.06E-3	3.21±1.15E-3	3.11±1.06E-3
R5 θ=10°-30°	3.18±7.67E-4	3.80±6.9E-4	3.21±7.63E-4	3.07±7.22E-4
R6 θ=30°-90°	3.07±7.55E-4	3.71±6.55E-4	3.11±7.47E-4	3.08±7.23E-4

Table 4.4 Slopes of the m_T spectra for the whole range and selected regions R1-R6 of the polar angle for 2GeV<m_T<3GeV

Polar Angle θ	N_{jet}=D	N_{jet}=0	N_{jet}=1	N_{jet}=2
whole range	1.87±0.01	4.61±0.01	1.77±0.02	1.95±0.01
R1 θ=0°-2°	1.17±0.06	3.99±0.05	0.76±0.14	1.68±0.02
R2 θ=2°-4°	1.98±0.04	4.64±0.07	1.99±0.04	1.93±0.03
R3 θ=4°-6°	1.96±0.05	4.58±0.06	1.93±0.05	1.97±0.04
R4 θ=6°-10°	1.77±0.04	4.44±0.06	1.88±0.05	2.10±0.03
R5 θ=10°-30°	1.67±0.04	4.14±0.07	1.79±0.03	1.89±0.02
R6 θ=30°-90°	1.85±0.03	4.22±0.05	1.86±0.03	1.84±0.02

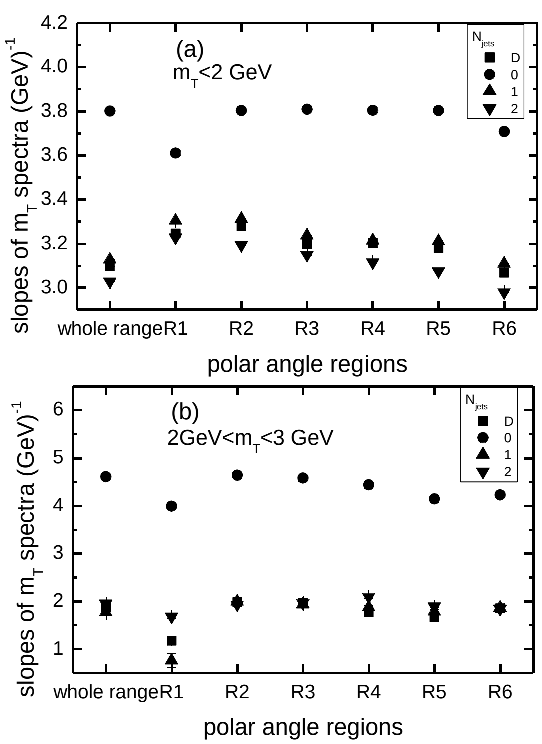

Figure 4.27 Slopes of the m_T spectra for the whole range and selected regions R1-R6 of the polar angle, (a) for m_T<2GeV and (b) for 2GeV<m_T<3GeV

Figure 4.27 (*(a)* and *(b)*) shows the plots of slopes of the m_T spectra for the whole range and selected six regions R1-R6 of polar angle for m_T<2GeV and for 2GeV<m_T<3GeV as a function of number of jets. Very similar behavior to Fig. 4.19 is seen here. Event selection with N_{jet}=0 affects the m_T distribution only up to m_T~3GeV, as for m_T>3GeV events with N_{jet}>0 are contributing.

For the above discussed three sections (4.4 to 4.6) we conclude the analysis of the effects of jet production on the pseudorapidity, transverse momentum and transverse mass distributions of secondary charged particles produced in *pp*-collisions at 1.8 TeV using the HIJING code. These distributions were analyzed for the whole range and for selected six regions of the polar angle as a function of different number of jets.

Some plateaus are observed in the central area of pseudorapidity. The existence of these plateaus is very important for the applicability of hydrodynamics. With increasing the number of jets the widths of the distributions decreased and the pseudorapidity density in the central area increased.

It was observed that with increasing the number of jets from 0 to 1, 2 or the default value of jets, the transverse momentum increased as the jets or multi-jet events contain high p_T particles.

The behavior of the p_T-distributions in the case of $N_{jet} \geq 1$ is different in two areas of p_T: p_T<2 GeV/c and p_T>2 GeV/c. The slopes of the distribution in the first area are very close to that for events with N_{jet}=0. We can therefore say that particles with p_T<2 GeV/c are produced by the same dynamics in events with different N_{jet}. The particles with p_T>2 GeV/c are those produced by some special dynamics, different from the particles with p_T<2 GeV/c. We may conclude that along with the multi-jet events, zero-jet events affect the p_T spectra only up to 3 GeV/c and for p_T>3GeV/c only the multi-jet events contribute. This is caused by the jet dynamics (production and hadronization of the jets) from the HIJING code. We also observed, in a previous study, similar results for the multiplicity distribution of charged particles. We concluded that the high multiplicity regions in the N_{ch} distribution correspond to multi-jet events.

Chapter 5 Conclusions

Here we summarize the conclusions.

We studied the effects of jet production on the multiplicity, pseudorapidity, transverse momentum and transverse mass distributions of charged particles produced in *pp*-collisions at 1.8 TeV, using the HIJING code. These distributions were analyzed for the whole range and for six selected regions (R1—R6) of the polar angle as a function of different number of jets.

The HIJING results show that there are three areas in multiplicity distributions of charged particles: $N_{ch}<15$, $15 < N_{ch}<80$ and $N_{ch}>80$. We identified the first area as a region dominating leading particles: elastic scattering region. The particles from this area correspond to the polar angle region R1 and without jets. The second region is contributed by multi-jet events along with zero jet events. The third area corresponds to multi-jet (1, 2 or more jets) events. Analysis of the multiplicity distributions for other angular regions (R2—R6) also showed that the increase in the charged particles multiplicity is connected to the multi-jet events.

We conclude that the high N_{ch} areas correspond to the multi-jet events. Our results were consistent with the analysis of weighted superposition mechanism of two negative binomial multiplicity distributions for hadronic collisions where the two components correspond to soft and semi-hard events respectively.

Some plateaus are observed in the central area of pseudorapidity. The existence of these plateaus is very important for the applicability of hydrodynamics. With increasing the number of jets the widths of the distributions decreased and the pseudorapidity density in the central area increased. From comparison of HIJING results with that of CDF we conclude that increase in the pseudorapidity density is due to multi-jet events.

It was observed that with increasing the number of jets (and the polar angle) the transverse momentum is increased as the jets or multi-jet events contain high p_T particles.

The behavior of the p_T–distributions for $N_{jet} \geq 1$ is different in two areas of p_T: p_T<2 GeV/c and p_T>2 GeV/c. The slopes of the distribution in the first area are very close to that for events with N_{jet}=0. We can therefore say that the particles with p_T<2 GeV/c are produced by the same dynamics in events with different N_{jet}. The particles with p_T>2 GeV/c are those produced by some special dynamics, different from the particles with p_T<2 GeV/c.

We may conclude that along with the multi-jet events, zero-jet events affect the p_T spectra only up to 3 GeV/c and for p_T>3GeV/c only the multi-jet events contribute. This is caused by the jet dynamics from the HIJING code. Analysis of transverse mass (m_T) distribution also showed a similar behavior to that of p_T distribution.

On the basis of this analysis we will continue further to study the effects of jet production/suppression in other hadronic collisions; hadron-nucleus and nucleus-nucleus collisions at the TeV energy scale.

References

[1] D. H. Perkins, Introduction to High Energy Physics, 4th Edition, Cambridge University Press, 2000.

[2] Fayyazuddin and Riazuddin, A Modern Introduction to Particle Physics, 3rd Edition, World Scientific Publishing, 2012.

[3] http://www.fnal.gov/pub/today/images/images11/NS_Figure01_2011_11_18.jpg

[4] H. Satz, Extreme State of Matter in Strong Interaction Physics - An Introduction, Springer, 2012.

[5] H. Satz, Colour deconfinement in nuclear collisions, Rep. Prog. Phys. **63** 1511–1574, 2000.

[6] J. Bartke, Introduction to Relativistic Heavy Ion Physics, World Scientific Publishing, 2009.

[7] R. Vogt, Ultrarelativistic Heavy-Ion Collisions, First Edition, Elsevier, 2007.

[8] B. Andersson et al., Parton Fragmentation and String Dynamics, Physics Reports **97**, (2–3), 31–145, 1983.

[9] G. Sterman, QCD and Jets, Yang Institute for Theoretical Physics, Stony Brook University Report YITP-SB-04-59, 2004.

[10] R. Hagedorn, Suppl. Nuovo. Cimento **3**, 3, p. 147, 1965.

[11] M. Gyulassy et al., Jet Quenching and Radiative Energy Loss in Dense Nuclear Matter, in R.C. Hwa & X.-N. Wang (eds.), Quark Gluon Plasma **3**, World Scientific, Singapore, 2003.

[12] S. Domdey, QCD Evolution of Jets in the Quark–Gluon Plasma, Nuclear Physics A **808**, 178–191, 2008.

[13] A. Sedrakian, J.W. Clark, M.G. Alford, Pairing in fermionic systems, World Scientific, 2007.

[14] S. D. Ellis and D. E. Soper, Successive Combination Jet Algorithm for Hadron Collisions, Phys. Rev. D **48**, 3160–3166, 1993.

[15] M. E. Peskin and D. V. Schroeder, An Introduction to Quantum Field Theory, Addison Wesley Publishing Company, 1995.

[16] A. A. Affolder et al. (CDF Collaboration), Phys. Rev. D **65**, 092002, 2002.

[17] Xin-Nian Wang, Jet and Leading Hadron Production in High-energy Heavy-ion Collisions, Nuclear Physics A **774**, 215–224, 2006.

[18] Y. I. Azimov, Y. L. Dokshitzer, V. A. Khoze, and S. I. Troian, Similarity of Parton and Hadron Spectra in QCD Jets, Z. Phys. C **27**, 65–72, 1985.

[19] Constantinos A. Loizides, Jet Physics in ALICE, arXiv:nucl-ex/0501017v3, 2005.

[20] G. C. Blazey et al., Run II Jet Physics, arXiv:hep-ex/0005012, 2000.

[21] G. Sterman and S. Weinberg, Jets from Quantum Chromodynamics, Phys. Rev. Lett. **39**, 1436, 1977.

[22] S. Bethke, Z. Kunszt, D. Soper, and W. J. Stirling, New Jet Cluster Algorithms: Next-to-Leading Order QCD and Hadronization Corrections, Nucl. Phys. B **370**, 310–334, 1992.

[23] S. Catani, Y. L. Dokshitzer, M. Olsson, G. Turnock, and B. R. Webber, New Clustering Algorithm for Multi-Jet Cross Sections in e+e− Annihilation, Phys. Lett., B **269**, 432–438, 1991.

[24] Y. L. Dokshitzer, G. D. Leder, S. Moretti, and B. R. Webber, Better Jet Clustering Algorithms, Journal of High Energy Physics **08**, 001, 1997.

[25] Matteo Cacciari, Gavin P. Salam and Gregory Soyez, The anti-k_t jet clustering algorithm, JHEP **04,** 063, 2008; arXiv:0802.1189v2 [hep-ph], 2008.

[26] G. Arnison et al., UA1 Collaboration, Observation of Jets in High Transverse Energy Events at the CERN proton–anti-proton Collider, Phys. Lett. B **123**, 115, 1983.

[27] F. Abe et al., CDF Collaboration, The Topology of Three Jet Events in pp Collisions at $\sqrt{s}$ = 1.8 TeV, Phys. Rev. D **45**, 1448–1458, 1992.

[28] S. D. Ellis, Z. Kunszt and E. D. Soper, Jets at Hadron Colliders at Order α_S^3: A Look Inside, Phys. Rev. Lett. **69**, 3615–3618, 1992.

[29] M. H. Seymour, Jet Shapes in Hadron Collisions: Higher Orders, Resummation and Hadronization, Nucl. Phys. B **513**, 269–300, 1998.

[30] S. D. Ellis, J. Huston, K. Hatakeyama, P. Loch and M. Tonnesmann, Jets in Hadron–Hadron Collisions, Progress in Particle and Nuclear Physics **60**, 484-551, 2008.

[31] J. L. Klay, Jet Measurements in the ALICE Experiment at the LHC, Nuclear Physics A **787**, 52c–59c, 2007.

[32] A. Ali and G. Kramer, Eur. Phys. J. H **36**, 245–326, 2011.

[33] G. Hanson et al., SLAC-LBL Collaboration, Evidence for Jet Structure in Hadron Production by e+e− Annihilation, Phys. Rev. Lett. **35**, 1609, 1975.

[34] G. Hanson et al., Hadron Production by e+e− Annihilation at Center-of-Mass Energies between 2.6 GeV and 7.8 GeV, Part 2: Jet Structure and Related Inclusive Distributions, Phys. Rev. D **26**, 991, 1982.

[35] J.D. Bjorken, S.J. Brodsky, Statistical Model for Electron-Positron Annihilation into Hadrons, Phys. Rev. D **1**, 1416, 1970.

[36] B. R. Martin, Nuclear and Particle Physics An Introduction, Wiley, 2006.

[37] R. Brandelik et al., TASSO Collaboration, Evidence for Planar Events in e+e− Annihilation at High Energies, Phys. Lett. B **86**, 243, 1979.

[38] D.P. Barber et al., Mark-J Collaboration, Discovery of Three Jet Events and a Test of Quantum Chromodynamics at Petra Energies, Phys. Rev. Lett. **43**, 830, 1979.

[39] C. Berger et al., PLUTO Collaboration, Evidence for Gluon Bremsstrahlung in e+e− Annihilations at High-Energies, Phys. Lett. B **86**, 418, 1979.

[40] W. Bartel et al., JADE Collaboration, Observation of Planar Three Jet Events in e+e− Annihilation and Evidence for Gluon Bremsstrahlung, Phys. Lett. B **91**, 142, 1980.

[41] B.H. Wiik, First Results From Petra, in Bergen 1979, Proceedings, Neutrino ’79, Vol.**1**, p. 113, 1979.

[42] J.R. Ellis, M.K. Gaillard, G.G. Ross, Search for Gluons in e+e− Annihilation, Nucl. Phys. B **111**, 253 (1976) [Erratum-ibid. B **130**, 516, 1977.

[43] S. Bethke, QCD studies at LEP, Phys. Rept. **203**, 403-404, 2004.

[44] A H Muller, Jets at LEP and HERA, J. Phys. G: Nucl. Part. Phys. **17**, 1443-1454, 1991.

[45] K. Hagiwara a,b, A.D. Martin a and W.J. Stirling, J/Psi production from gluon jets at LEP, Physics Letters B **267**, 527-531, 1991.

[46] A. Breakstone et al., Ames-Bologna-CERN-Dortmund-Heidelberg-Warsaw Collaboration, High p_T Hadrons as Leading Particles in Jets Produced at the ISR; 1- Momentum Distribution of Secondaries in the Trigger Jet, Z. Phys. C **23**, 9. 1984.

[47] R.D. Field, R.P. Feynman, A Parameterization of the Properties of Quark Jets, Nucl. Phys. B **136**, 1, 1978.

[48] F. Abe et al., CDF Collaboration, Phys. Rev. Lett. **73**, 225 1994.

[49] F. Abe et al., CDF Collaboration, Phys. Rev. Lett. **74**, 2626 1995.

[50] S. Abachi et al., D0 Collaboration, Phys. Rev. Lett. **74**, 2632 1995.

[51] S. Salur, Jet Reconstruction in Heavy Ion Collisions, 25^{th} Winter Workshop on Nuclear Dynamics Proceedings, Big Sky, Montana, arXiv:0905.1917, 2009.

[52] L. C. Bland, for the A_NDY Collaboration, Measurement of Forward Jets at RHIC, arXiv:1308.4705v1 [hep-ex], 2013.

[53] F. Antinori, Heavy-Ion Physics with ALICE, Nuclear Physics B (Proc. Suppl.) **177–178**, 156–160, 2008.

[54] http://education.web.cern.ch/education/images/LHC_Event_BH_ATLAS.jpg

[55] Pierre Van Mechelen, Jet Production in ep Collisions, arXiv:hep-ex/0305073v1, 2003.

[56] C. Adloff et al., H1 Collaboration, Measurement of Inclusive Jet Cross-Section in Deep-Inelastic ep Scattering at HERA, Phys. Lett. B **542**, 193, 2002.

[57] S. Chekanov et al., ZEUS Collaboration, Inclusive Jet Cross-Section in the Breit Frame in Neutral Current Deep-Inelastic Scattering at HERA and Determination of α_s, Phys. Lett. B **547**, 164, 2002.

[58] The OPAL Collaboration, Di-Jet Production in Photon-Photon Collisions at $\sqrt{s_{ee}}$ = 161 and 172 GeV, CERN-EP/98-113, 1998.

[59] T. Sjöstrand et al., Pythia 6.3 Physics and Manual, Department of Theoretical Physics, Lund University Report LUTP 03-38, 2003.

[60] J. Breitweg et al., ZEUS Collaboration. High-E_T Inclusive Jet Cross-Sections in Photo-production at HERA, DESY-98-018, 1998.

[61] K. Ackerstaff et al., OPAL Collaboration, Inclusive Jet Production in Photon-Photon Collisions at $\sqrt{s_{ee}}$ = 130 and 136 GeV, Z. Phys. C **73**, 433, 1997.

[62] F. Hautmann and H. Jung, Angular Correlations in Multi-Jet Final States from $k_\perp$ dependent Parton Showers, arXiv: 0805.1049v3 [hep-ph], 2008.

[63] A. Majumder and M. van Leeuwen, Prog. Part. Nucl. Phys., **66**, 41-92, 2011.

[64] M. Spousta, Mod. Phys. Lett. A, **28**, 1330017, 2013.

[65] M. Gyulassy, M. Plumer, Jet quenching in dense matter, Phys. Lett. B **243**, 432–438, 1990.

[66] F. Antinori et al., NA57 Collaboration, Central-to-peripheral nuclear modification factors in Pb–Pb collisions at $\sqrt{s_{NN}}$ = 17.3 GeV, Physics Letters B **623**, 17–25, 2005.

[67] ALICE Collaboration, Measurement of jet suppression in central Pb–Pb collisions at $\sqrt{s_{NN}}$=2.76 TeV', Physics Letters B Vol. **746**, 1–14, 2015.

[68] BRAHMS Collaboration, I. Arsene, et al., Quark–gluon plasma and color glass condensate at RHIC? The perspective from the BRAHMS experiment, Nucl. Phys. A **757**, (1–2), 1–27, 2005.

[69] PHOBOS Collaboration, B. Back, et al., The PHOBOS perspective on discoveries at RHIC, Nucl. Phys. A **757**, (1–2), 28–101, 2005.

[70] PHENIX Collaboration, K. Adcox, et al., Formation of dense partonic matter in relativistic nucleus–nucleus collisions at RHIC: experimental evaluation by the PHENIX Collaboration, Nucl. Phys. A **757**, (1–2), 184–283, 2005.

[71] STAR Collaboration, J. Adams, et al., Experimental and theoretical challenges in the search for the quark–gluon plasma: the STAR Collaboration's critical assessment of the evidence from RHIC collisions, Nucl. Phys. A **757**, (1–2) , 102–183, 2005.

[72] ALICE Collaboration, K. Aamodt, et al., Charged-particle multiplicity density at mid-rapidity in central Pb–Pb collisions at $\sqrt{s_{NN}}$=2.76 TeV, Phys. Rev. Lett. **105**, 252301, 2010.

[73] ALICE Collaboration, K. Aamodt, et al., Centrality dependence of the charged-particle multiplicity density at mid-rapidity in Pb–Pb collisions at $\sqrt{s_{NN}}$=2.76 TeV, Phys. Rev. Lett. **106**, 032301, 2011.

[74] CMS Collaboration, S. Chatrchyan, et al., Dependence on pseudorapidity and centrality of charged hadron production in Pb–Pb collisions at a nucleon–nucleon centre-of-mass energy of 2.76 TeV, J. High Energy Phys. **1108**, 141, 2011.

[75] ALICE Collaboration, K. Aamodt, et al., Two-pion Bose–Einstein correlations in central Pb–Pb collisions at $\sqrt{s_{NN}}$=2.76 TeV, Phys. Lett. B **696**, 328–337, 2011.

[76] ALICE Collaboration, K. Aamodt, et al., Elliptic flow of charged particles in Pb–Pb collisions at 2.76 TeV, Phys. Rev. Lett. **105**, 252302, 2010.

[77] ATLAS Collaboration, G. Aad, et al., Measurement of the pseudorapidity and transverse momentum dependence of the elliptic flow of charged particles in lead–lead collisions at $\sqrt{s_{NN}}$=2.76 TeV with the ATLAS detector, Phys. Lett. B **707**, 330–348, 2012.

[78] CMS Collaboration, S. Chatrchyan, et al., Centrality dependence of dihadron correlations and azimuthal anisotropy harmonics in Pb–Pb collisions at $\sqrt{s_{NN}}$=2.76 TeV, Eur. Phys. J. C **72**, 2012, 2012.

[79] ALICE Collaboration, K. Aamodt, et al., Higher harmonic anisotropic flow measurements of charged particles in Pb–Pb collisions at $\sqrt{s_{NN}}$=2.76 TeV, Phys. Rev. Lett. **107**, 032301, 2011.

[80] ATLAS Collaboration, G. Aad, et al., Measurement of the distributions of event-by-event flow harmonics in lead–lead collisions at 2.76 TeV with the ATLAS detector at the LHC, J. High Energy Phys. **1311**, 183, 2013.

[81] CMS Collaboration, S. Chatrchyan, et al., Measurement of higher-order harmonic azimuthal anisotropy in Pb–Pb collisions 2.76 TeV, Phys. Rev. C **89**, 044906, 2014.

[82] ALICE Collaboration, K. Aamodt, et al., Suppression of charged particle production at large transverse momentum in central Pb–Pb collisions at 2.76 TeV, Phys. Lett. B **696**, 30–39, 2011.

[83] CMS Collaboration, S. Chatrchyan, et al., Observation and studies of jet quenching in Pb–Pb collisions at nucleon–nucleon center-of-mass energy of 2.76 TeV, Phys. Rev. C **84**, 024906, 2011.

[84] PHENIX Collaboration, K. Adcox, et al., Suppression of hadrons with large transverse momentum in central Au+Au collisions at 130 GeV, Phys. Rev. Lett. **88**, 022301, 2002.

[85] STAR Collaboration, C. Adler, et al., Disappearance of back-to-back high p_T hadron correlations in central Au+Au collisions at $\sqrt{s_{NN}}$=200 GeV, Phys. Rev. Lett. **90**, 082302, 2003.

[86] PHENIX Collaboration, K. Adcox, et al., Centrality dependence of the high-p_T charged hadron suppression in Au+Au collisions at $\sqrt{s_{NN}}$=130 GeV, Phys. Lett. B **561**, 82–92, 2003.

[87] PHENIX Collaboration, S.S. Adler, et al., Suppressed π^0 production at large transverse momentum in central Au+Au collisions at 200 GeV, Phys. Rev. Lett. **91**, 072301, 2003.

[88] STAR Collaboration, J. Adams, et al., Transverse-momentum and collision-energy dependence of high-p_T hadron suppression in Au+Au collisions at ultrarelativistic energies, Phys. Rev. Lett. **91**, 172302, 2003.

[89] STAR Collaboration, J. Adams, et al., Evidence from d+Au measurements for final state suppression of high-p_T hadrons in Au+Au collisions at RHIC, Phys. Rev. Lett. **91**, 072304, 2003.

[90] PHOBOS Collaboration, B. Back, et al., Charged hadron transverse momentum distributions in Au+Au collisions at 200 GeV, Phys. Lett. B **578**, 297–303, 2004.

[91] BRAHMS Collaboration, I. Arsene, et al., Transverse momentum spectra in Au+Au and d+Au collisions at $\sqrt{s_{NN}}$=200 GeV and the pseudorapidity dependence of high-p_T suppression, Phys. Rev. Lett. **91**, 072305, 2003.

[92] PHENIX Collaboration, A. Adare, et al., System size and energy dependence of jet-induced hadron pair correlation shapes in Cu+Cu and Au+Au collisions at $\sqrt{s_{NN}}$=200 and 62.4 GeV, Phys. Rev. Lett. **98**, 232302, 2007.

[93] PHENIX Collaboration, A. Adare, et al., Quantitative constraints on the opacity of hot partonic matter from semi-inclusive single high transverse momentum pion suppression in Au+Au collisions at $\sqrt{s_{NN}}$=200 GeV, Phys. Rev. C **77**, 064907, 2008.

[94] ATLAS Collaboration, G. Aad, et al., Observation of a centrality-dependent dijet asymmetry in Pb–Pb collisions at $\sqrt{s_{NN}}$=2.76 TeV with the ATLAS detector at the LHC, Phys. Rev. Lett. **105**, 252303, 2010.

[95] ALICE Collaboration, K. Aamodt, et al., Particle-yield modification in jet-like azimuthal di-hadron correlations in Pb–Pb collisions at $\sqrt{s_{NN}}$=2.76 TeV, Phys. Rev. Lett. **108**, 092301, 2012.

[96] CMS Collaboration, S. Chatrchyan, et al., Study of high-p_T charged particle suppression in Pb–Pb compared to pp collisions at $\sqrt{s_{NN}}$=2.76 TeV, Eur. Phys. J. C **72**, 1945, 2012.

[97] CMS Collaboration, S. Chatrchyan, et al., Jet momentum dependence of jet quenching in Pb–Pb collisions at $\sqrt{s_{NN}}$=2.76 TeV, Phys. Lett. B **712**, 176–197, 2012.

[98] CMS Collaboration, S. Chatrchyan, et al., Measurement of jet fragmentation into charged particles in pp and Pb–Pb collisions at $\sqrt{s_{NN}}$=2.76 TeV, J. High Energy Phys. **1210**, 087, 2012.

[99] CMS Collaboration, S. Chatrchyan, et al., Studies of jet quenching using isolated photon+jet correlations in Pb–Pb and pp collisions at $\sqrt{s_{NN}}$=2.76 TeV, Phys. Lett. B **718**, 773–794, 2013.

[100] ATLAS Collaboration, G. Aad, et al., Measurement of the jet radius and transverse momentum dependence of inclusive jet suppression in lead–lead collisions at $\sqrt{s_{NN}}$=2.76 TeVwith the ATLAS detector, Phys. Lett. B **719**, 220–241, 2013.

[101] CMS Collaboration, S. Chatrchyan, et al., Evidence of b-jet quenching in Pb–Pb collisions at $\sqrt{s_{NN}}$=2.76 TeV, Phys. Rev. Lett. **113**, (13), 132301, 2014.

[102] CMS Collaboration, S. Chatrchyan, et al., Modification of jet shapes in Pb–Pb collisions at $\sqrt{s_{NN}}$=2.76 TeV, Phys. Lett. B **730**, 243–263, 2014.

[103] CMS Collaboration, S. Chatrchyan, et al., Measurement of jet fragmentation in Pb–Pb and pp collisions at $\sqrt{s_{NN}}$=2.76 TeV, arXiv:1406.0932 [nucl-ex]. 2014.

[104] ATLAS Collaboration, G. Aad, et al., Measurement of inclusive jet charged-particle fragmentation functions in Pb+Pb collisions at $\sqrt{s_{NN}}$=2.76 TeV with the ATLAS detector, arXiv:1406.2979 [hep-ex]. 2014.

[105] ATLAS Collaboration, G. Aad, et al., Measurements of the nuclear modification factor for jets in Pb–Pb collisions at $\sqrt{s_{NN}}$=2.76 TeV with the ATLAS detector, arXiv:1411.2357 [hep-ex]. 2014.

[106] https://www.star.bnl.gov/central/focus/highPt/

[107] A. Adare, et al., PHENIX Collaboration, Phys. Rev. C **78**, 014901, 2008.

[108] J. Adams, et al., Star Collaboration, Nucl. Phys. A **757**, 102, 2005.

[109] V. V. Uzhinsky, arXiv:hep-ph/0312089v2, 2003.

[110] http://hepweb.jinr.ru/hijing_0_1/.

[111] Roberto Ugoccioni and Alberto Giovannini, Scenarios for multiplicity distributions in pp collisions in the TeV energy region, Journal of Physics: Conference Series **5**, 199–208, 2005.

[112] X-. N. Wang and M. Gyulassy, Phys. Rev. D **44**, 3501, 1991.

[113] http://www-nsdth.lbl.gov/~xnwang/hijing/ .

[114] M. Gyulassy and X-. N. Wang, Comp. Phys. Commun. **83**, 307, 1994.

[115] M. Manner et al., Phys. Lett. B **118**, 203, 1982.

[116] C. Albajar et al., Nucl. Phys. B **309**, 405, 1988.

[117] C. Albajar et al., Nuci. Phys. B **335**, 261, 1990.

[118] A. Capella and J. Tran Thanh Van, Z. Phys. C **23**, 165, 1984.

[119] Ali Zaman, Mais Suleymanov, Muhammad Ajaz and Kamal Hussain Khan, Int. J. Mod. Phys. E, **23**, 1450029, 2014.

[120] Ali Zaman, Mais Suleymanov, Muhammad Ajaz and Kamal Hussain Khan, Chinese Physics C, **39**, 073001, 2015.

[121] J. D. Bjorken, FERMILAB-PUB-82-059-THY, 1982.

[122] S. S. Adler, et al., PHENIX Collaboration, Phys. Rev. C **69**, 034910, 2004.

[123] D. d'Enterria, Phys. Lett. B **596**, 32, 2004.

[124] David R. Harrington, Multiple Scattering, the Glauber Approximation, and the Off-Shell Eikonal Approximation, Physical Review **184**, 5, 1969.

[125] G. J. Alner et al., UA5 Collaboration, Physics Reports **154**, 247, 1987.

[126] R. E. Ansorge et al., UA5 Collaboration, Z. Phys. C **43**, 357, 1989.

[127] Sandor Hegyi, KNO scaling 30 years later, arXiv:hep-ph/0011301v1, 2000.

[128] A. M. Polyakov, A similarity hypothesis in the strong interactions, I. Multiple hadron production in e+e- annihilation, Soviet Physics JETP **32**, 1, 1971.

[129] L. L. Jenkovszky and B. V. Struminsky, On the Distribution of Secondaries at High Energies, arXiv:hep-ph/0205322v2, 2002.

[130] T. Alexopoulos et al., E735 Collaboration, Phys. Lett. B **435**, 453, 1998.

[131] M. Biyajima, T. Mizoguchi, N. Nakajima, A. Ohsawa and N. Suzuki, Analyses of multiplicity distributions at Tevatron by a two-component stochastic Model -No leading particle effect in E735 Experiment-, arXiv:hep-ph/0106016v2, 2001.

[132] T. Mizoguchi, M. Biyajima and G. Wilk, Phys. Lett. B **301**, 131, 1993.

[133] T. Mizoguchi, T. Aoki, M. Biyajima and N. Suzuki, Prog. Theor. Phys. **88**, 391, 1992.

[134] M. Ajaz, M. K. Suleymanov, K. H. Khan, Ali Zaman, H. Younas and A. Rahman, Mod. Phys. Lett. A **28**, 1350175, 2013.

[135] M. Ajaz M. K. Suleymanov, K. H. Khan and Ali Zaman, Int. J. Mod. Phys. E **21**, 1250095, 2012.

[136] F. Abe et al., CDF Collaboration, Phys. Rev. D, **41**, 2330(R), 1990.

[137] J. D. Bjorken, Phys. Rev. D **27,** 140-151, 1983.

[138] A. Mueller, in Proceedings of the 1981 ISABELLE Summer Workshop, edited by H. Gordon, BNL, Upton, New York, 636, 1982.

List of Publications of Ali Zaman

This Thesis is particularly based on the first two papers.

1. Ali Zaman, Mais Suleymanov, Muhammad Ajaz and Kamal Hussain Khan, "Effect of the Jet Production on Pseudorapidity, Transverse Momentum and Transverse Mass Distributions of Charged Particles Produced in *pp*-Collisions at Tevatron Energy", Chinese Physics C, Vol. **39**, No. 7, 073001, 2015
2. Ali Zaman, Mais Suleymanov, Muhammad Ajaz and Kamal Hussain Khan, "On influences of the jet production to charged particles multiplicity distribution in pp-collisions at Tevatron energies", International Journal of Modern Physics E, Vol. **23**, No. 5, 1450029, 2014
3. Kamal Hussain Khan, M. K. Suleymanov, M. Ajaz, Ali Zaman, H. Younis, "The study of light nuclei production in different interactions at 4.2 AGeV/c", Canadian Journal of Physics, Vol. **94** (2016)
4. M. Ajaz, M. K. Suleymanov, K. H. Khan, Ali Zaman, H. Younis, Z. Wazir and Bahar Ali, "Average characteristic of π^--mesons in HeC and CC interactions at high energies", International Journal of Modern Physics E, Vol. **25**, No. 3, 1650019, 2016
5. K. H. Khan, M. K. Suleymanov, M. Ajaz, Ali Zaman and Sh. Khalilova, "Light nuclei formation in ^{12}CC collisions at 4.2 A GeV/c ", Modern Physics Letters A, Vol. **29**, No. 12, 1450063, 2014
6. M. Ajaz, M. K. Suleymanov, K. H. Khan, Ali Zaman, H. Younis and A. Rahman, "Study of some characteristics of protons using interactions of light nuclei", Modern Physics Letters A, Vol. **28**, No. 37, 1350175, 2013
7. Muhammad Ajaz, Mais K Suleymanov, Kamal Hussain Khan and Ali Zaman, "Nuclear transparency effect of π^--mesons in p+^{12}C- and d+^{12}C- interactions at 4.2 A GeV/c", Journal of Physics G: Nuclear and Particle Physics, Vol. **40**, 055101, 2013
8. M. Ajaz, M. K. Suleymanov, K. H. Khan, Ali Zaman, "Study of the behavior of the nuclear modification factor in freeze-out state", Chinese Physics C, Vol. **37**, No. 2, 024101, 2013

9. M. Ajaz, M. K. Suleymanov, K. H. Khan and Ali Zaman, "Searching For the Properties of Nuclear Matter Using Proton-Carbon and Deuteron-Carbon Collisions at 4.2 *A* GeV/c", International Journal of Modern Physics E, Vol. **21**, No. 12, 1250095, 2012
10. M. Ajaz, M. K. Suleymanov, O. B. Abdinov, Ali Zaman, K. H. Khan, Z. Wazir, Sh. Khalilova, "Nuclear Transparency Effect in the Strongly Interacting Matter", Fizika, Vol. **XVII**, No. 3, 17-20, 2011
11. B. Z. Belashev, M. K. Suleymanov, S. Vokal, J. Vrlakova, M. Ajaz, Ali Zaman, K. H. Khan, Z. Wazir, "Analysis of Shower Particle Pseudorapidity Spectra in Interactions of Relativistic Au and Pb Ions with Emulsion Nuclei", Chinese Physics C, CPC(HEP & NP), Vol. **35**, No. 12, 1095-1099, 2011

Conference Proceedings

12. M. K. Suleymanov, R. G. Nazmitdinov, E. I. Shahaliev, O. B. Abdinov, M. Ajaz, Ali Zaman, K. H. Khan, Z. Wazir, "Applying a new method for analyzing experimental data on nuclear reactions at high energies", Bulletin of the Russian Academy of Sciences: Physics, Vol. **76**, No. 10, 1089-1092, 2012
13. M. K. Suleymanov, B. Z. Belashev, S. Vokal, A. S. Vodopianov, J. Vrláková, O. B. Abdinov, M. Ajaz, Ali Zaman, K. H. Khan and Sh. Khalilova, "Pseudorapidity spectra of secondary particles emitted in the relativistic nucleus-nucleus collisions", Proceedings of Science PoS (Baldin ISHEPP XXI) 043, 2012
14. K. H. Khan, M. K. Suleymanov, M. Ajaz, Ali Zaman and Sh. Khalilova, "Observation of light nuclei formation as nuclear coalescence in CC-interactions at 4.2 A GeV/c ", Proceedings of Science PoS (Baldin ISHEPP XXI) 045, 2012
15. M. Ajaz, M. K. Suleymanov, K. H. Khan, Ali Zaman and Sh. Khalilova, "Nuclear transparency effect in proton and deuteron induced interactions with carbon nuclei", Proceedings of Science PoS (Baldin ISHEPP XXI) 052, 2012
16. M. Ajaz, M. K. Suleymanov, Ali Zaman, K. H. Khan, Z. Wazir, Proceedings of the XX International Baldin Seminar on High Energy Physics Problems "Relativistic

Nuclear Physics & Quantum Chromodynamics", 2011, e-Print: arXiv:1101.2767 [nucl-ex]

17. B. Z. Belashev, M. K. Suleymanov, S. Vokál, J. Vrláková, M. Ajaz, K. H. Khan, Ali Zaman, Z. Wazir, Proceedings of the XX International Baldin Seminar on High Energy Physics Problems "Relativistic Nuclear Physics & Quantum Chromodynamics", 2011, e-Print: arXiv:1101.4252 [nucl-ex]
18. M. K. Suleymanov, M. Ajaz, Ali Zaman, K. H. Khan, Z. Wazir, "High Density and/or High Temperature Nuclear Matter may be a Source of High Energy Cosmic Particles", Proceedings of Science PoS (EPS-HEP 2009) 406, 2009

MS Thesis published as book

19. Ali Zaman, "Jets in High Energy Hadronic Collisions: Jet Production in Hadron-Nucleus and Nucleus-Nucleus Collisions at Relativistic and Ultrarelativistic Energies", LAP Lambert Academic Publishing GmbH & Co. KG, Germany, 2011. ISBN # 9783843380935

Publications with the ALICE Collaboration (LHC CERN Switzerland)

1. ALICE Collaboration, "Centrality dependence of ψ(2S) suppression in p-Pb collisions at 5.02 TeV", JHEP **06** (2016) 50
2. ALICE Collaboration, "Centrality dependence of the charged-particle multiplicity density at mid-rapidity in Pb-Pb collisions at 5.02 TeV", Phys. Rev. Lett. **116** (2016) 222302
3. ALICE Collaboration, "Differential studies of inclusive J/ψ and ψ(2S) production at forward rapidity in Pb-Pb collisions at 2.76 TeV", JHEP **05** (2016) 179
4. ALICE Collaboration, "Particle identification in ALICE: a Bayesian approach", Eur. Phys. J. Plus **131** (2016) 168
5. ALICE Collaboration, "Centrality dependence of charged jet production in p-Pb collisions at 5.02 TeV", Eur. Phys. J. C **76** (2016) 271
6. ALICE Collaboration, "Multi-strange baryon production in p-Pb collisions at 5.02 TeV", Phys. Lett. B **758** (2016) 389-401

7. ALICE Collaboration, “Production of K*(892) and φ(1020) in p-Pb collisions at 5.02 TeV”, Eur. Phys. J. C **76** (2016) 245
8. ALICE Collaboration, “Charge-dependent flow and the search for the Chiral Magnetic Wave in Pb-Pb collisions at 2.76 TeV”, Phys. Rev. C **93** (2016) 044903
9. ALICE Collaboration, “Inclusive quarkonium production at forward rapidity in pp collisions at 8 TeV”, Eur. Phys. J. C **76** (2016) 184
10. ALICE Collaboration, “Anisotropic flow of charged particles in Pb-Pb collisions at 5.02 TeV”, Phys. Rev. Lett. **116** (2016) 132302
11. ALICE Collaboration, “Event shape engineering for inclusive spectra and elliptic flow in Pb-Pb collisions at 2.76 TeV”, Phys. Rev. C **93** (2016) 034916
12. ALICE Collaboration, “Centrality dependence of the nuclear modification factor of charged pions, kaons, and protons in Pb-Pb collisions at 2.76 TeV”, Phys. Rev. C **93** (2016) 034913
13. ALICE Collaboration, “Transverse momentum dependence of D-meson production in Pb-Pb collisions at 2.76 TeV”, JHEP **03** (2016) 081
14. ALICE Collaboration, “Measurement of D+ production and nuclear modification factor in Pb-Pb collisions at 2.76 TeV”, JHEP **03** (2016) 082
15. ALICE Collaboration, “Multipion Bose-Einstein correlations in pp, p-Pb, and Pb-Pb collisions at the LHC”, Phys. Rev. C **93** (2016) 054908
16. ALICE Collaboration, “Production of light nuclei and anti-nuclei in pp and Pb-Pb collisions at energies available at the CERN Large Hadron Collider”, Phys. Rev. C **93** (2016) 024917
17. ALICE Collaboration, “Centrality dependence of pion freeze-out radii in Pb-Pb collisions at $\sqrt{s_{NN}}$=2.76 TeV”, Phys. Rev. C **93** (2016) 024905
18. ALICE Collaboration, “Direct photon production in Pb–Pb collisions at $\sqrt{s_{NN}}$=2.76 TeV”, Phys. Lett. B **754** (2016) 235-248
19. ALICE Collaboration, “ ${}^{3}_{\Lambda}H$ and ${}^{3}_{\Lambda}\overline{H}$ production in Pb-Pb collisions at $\sqrt{s_{NN}}$=2.76 TeV”, Phys. Lett. B **754** (2016) 360-372
20. ALICE Collaboration, “Centrality evolution of the charged-particle pseudorapidity density over a broad pseudorapidity range in Pb-Pb collisions at $\sqrt{s_{NN}}$=2.76 TeV”, Phys. Lett. B **754** (2016) 373-385

21. ALICE Collaboration, “Forward-central two-particle correlations in p-Pb collisions at $\sqrt{s_{NN}}$=5.02 TeV”, Phys. Lett. B **753** (2016) 126-139
22. ALICE Collaboration, “Study of cosmic ray events with high muon multiplicity using the ALICE detector at the CERN Large Hadron Collider”, Journal of Cosmology and Astroparticle Physics **01** (2016) 032
23. ALICE Collaboration, “Azimuthal anisotropy of charged jet production in $\sqrt{s_{NN}}$=2.76 TeV Pb-Pb collisions”, Phys. Lett. B **753** (2016) 511-525
24. ALICE Collaboration, “Pseudorapidity and transverse-momentum distributions of charged particles in proton-proton collisions at $\sqrt{s}$ =13 TeV”, Phys. Lett. B **753** (2016) 319-329
25. ALICE Collaboration, “Centrality dependence of high-p_T D meson suppression in Pb-Pb collisions at $\sqrt{s_{NN}}$=2.76 TeV”, JHEP **11** (2015) 205
26. ALICE Collaboration, “One-dimensional pion, kaon, and proton femtoscopy in Pb-Pb collisions at $\sqrt{s_{NN}}$=2.76 TeV”, Phys. Rev. C **92** (2015) 054908
27. ALICE Collaboration, “Centrality dependence of inclusive J/ψ production in p-Pb collisions at $\sqrt{s_{NN}}$=5.02 TeV”, JHEP **11** (2015) 127
28. ALICE Collaboration, “Coherent ψ(2S) photo-production in ultra-peripheral Pb-Pb collisions at $\sqrt{s_{NN}}$= 2.76 TeV”, Phys. Lett. B **751** (2015) 358-370
29. ALICE Collaboration, “Measurement of jet quenching with semi-inclusive hadron-jet distributions in central Pb-Pb collisions at $\sqrt{s_{NN}}$=2.76 TeV”, JHEP **09** (2015) 170
30. ALICE Collaboration, “Measurement of charm and beauty production at central rapidity versus charged-particle multiplicity in proton-proton collisions at $\sqrt{s}$=7 TeV”, JHEP **09** (2015) 148
31. ALICE Collaboration, “Coherent ρ^0 photoproduction in ultra-peripheral Pb--Pb collisions at $\sqrt{s_{NN}}$=2.76 TeV”, JHEP **09** (2015) 095
32. ALICE Collaboration, “Measurement of charged jet production cross sections and nuclear modification in p-Pb collisions at $\sqrt{s_{NN}}$=5.02 TeV”, Phys. Lett. B **749** (2015) 68-81
33. ALICE Collaboration, “Precision measurement of the mass difference between light nuclei and anti-nuclei”, Nature Physics **11** (2015) 811–814

34. ALICE Collaboration, “Inclusive, prompt and non-prompt J/ψ production at mid-rapidity in Pb-Pb collisions at $\sqrt{s_{NN}}$= 2.76 TeV”, JHEP **07** (2015) 051
35. ALICE Collaboration, “Elliptic flow of identified hadrons in Pb-Pb collisions at $\sqrt{s_{NN}}$=2.76 TeV”, JHEP **06** (2015) 190
36. ALICE Collaboration, “Charged jet cross sections and properties in proton-proton collisions at $\sqrt{s}$=7 TeV”, Phys. Rev. D **91** (2015) 112012
37. ALICE Collaboration, “Rapidity and transverse-momentum dependence of the inclusive J/ψ nuclear modification factor in p-Pb collisions at $\sqrt{s_{NN}}$=5.02 TeV”, JHEP **06** (2015) 55
38. ALICE Collaboration, “Centrality dependence of particle production in p-Pb collisions at $\sqrt{s_{NN}}$=5.02 TeV”, Phys. Rev. C **91** (2015) 064905
39. ALICE Collaboration, “Measurement of pion, kaon and proton production in proton-proton collisions at $\sqrt{s}$=7 TeV’’, Eur. Phys. J. C **75** (2015) 226
40. ALICE Collaboration, “Forward-backward multiplicity correlations in pp collisions at $\sqrt{s}$=0.9, 2.76 and 7 TeV’’, Journal of High Energy Physics, **05** (2015) 097
41. ALICE Collaboration, “Measurement of jet suppression in central Pb–Pb collisions at $\sqrt{s_{NN}}$=2.76 TeV’’, Physics Letters B Vol. **746** (2015) 1–14
42. ALICE Collaboration, “Inclusive photon production at forward rapidities in proton-proton collisions at $\sqrt{s}$ =0.9, 2.76 and 7 TeV’’, Eur. Phys. J. C **75** (2015) 146
43. ALICE Collaboration, “Two-pion femtoscopy in p-Pb collisions at $\sqrt{s_{NN}}$=5.02 TeV” Phys. Rev. C **91** (2015) 034906
44. ALICE Collaboration, “K*(892)0 and phi(1020) production in Pb-Pb collisions at $\sqrt{s_{NN}}$=2.76 TeV”, Phys. Rev. C **91** (2015) 024609
45. ALICE Collaboration, “Production of Σ(1385)± and Ξ(1530)0 in proton-proton collisions at $\sqrt{s}$=7 TeV’’, Eur. Phys. J. C **75** (2015) 1
46. ALICE Collaboration, “Measurement of electrons from semi-leptonic heavy-flavour hadron decays in proton-proton collisions at sqrt(s) = 2.76 TeV with ALICE’’, Phys. Rev. D **91** (2015) 012001
47. ALICE Collaboration, “Multiplicity dependence of jet-like two-particle correlations in pPb collisions at $\sqrt{s_{NN}}$=5.02 TeV with ALICE at LHC’’, Physics Letters B **741** (2015) 38–50

48. ALICE Collaboration, “Production of inclusive ϒ (1S) and ϒ (2S) in p–Pb collisions at $\sqrt{s_{NN}}$=5.02 TeV’’, Physics Letters B **740** (2015) 105–117
49. ALICE Collaboration, “Suppression of psi(2S) production in p-Pb collisions at $\sqrt{s_{NN}}$=5.02 TeV’’, Journal of High Energy Physics, **12** (2014) 073
50. ALICE Collaboration, “Measurement of prompt D-meson production in p–Pb collisions at $\sqrt{s_{NN}}$=5.02 TeV’’, Phys. Rev. Lett. **113** (2014) 232301
51. ALICE Collaboration, “Exclusive J/ψ photoproduction off protons in ultra-peripheral p-Pb collisions at $\sqrt{s_{NN}}$=5.02 TeV’’, Phys. Rev. Lett. **113** (2014) 232504
52. ALICE Collaboration, “Measurement of visible cross sections in proton-lead collisions at $\sqrt{s_{NN}}$=5.02 TeV in van der Meer scans with the ALICE detector’’, JINST **9** (2014) 1100
53. ALICE Collaboration, “Multi-particle azimuthal correlations in p-Pb and Pb-Pb collisions at the CERN Large Hadron Collider’’, Phys. Rev. C **90** (2014) 054901
54. ALICE Collaboration, “Freeze-out radii extracted from three-pion cumulants in pp, p-Pb and Pb-Pb collisions at the LHC’’, Physics Letters B **739** (2014) 139–151
55. ALICE Collaboration, “Neutral pion production at midrapidity in pp and PbPb collisions at $\sqrt{s_{NN}}$=2.76 TeV’’, Eur. Phys. J. C **74** (2014) 3108
56. ALICE Collaboration, “Event-by-event mean p_T fluctuations in pp and Pb-Pb collisions at the LHC’’, Eur. Phys. J. C **74** (2014) 3077
57. ALICE Collaboration, “Suppression of Upsilon(1S) at forward rapidity in Pb-Pb collisions at $\sqrt{s_{NN}}$=2.76 TeV”, Physics Letters B **738** (2014) 361-372
58. ALICE Collaboration, “Performance of the ALICE experiment at the CERN LHC”, Int. J. Mod. Phys. A **29** (2014) 1430044
59. ALICE Collaboration, “Beauty production in pp collisions at $\sqrt{s_{NN}}$=2.76 TeV measured via semi-electronic decays”, Physics Letters B **738** (2014) 97-108
60. ALICE Collaboration, “Transverse momentum dependence of inclusive primary charged-particle production in pPb collisions at $\sqrt{s_{NN}}$=5.02 TeV”, The European Physical Journal C **74** (2014) 3054
61. ALICE Collaboration, “Azimuthal anisotropy of *D*-meson production in Pb-Pb collisions at $\sqrt{s_{NN}}$=2.76 TeV”, Physical Review C **90** (2014) 034904

62. ALICE Collaboration, “Measurement of quarkonium production at forward rapidity in pp collisions at $\sqrt{s}$=7 TeV”, The European Physical Journal C **74** (2014) 2974
63. ALICE Collaboration, “Production of charged pions, kaons and protons at large transverse moment in pp and Pb-Pb collisions at $\sqrt{s_{NN}}$=2.76 TeV”, Physics Letters B **736** (2014) 196-207
64. ALICE Collaboration, “Centrality, rapidity and transverse momentum dependence of J/psi suppression in Pb-Pb collisions at $\sqrt{s_{NN}}$=2.76 TeV”, Physics Letters B **734** (2014) 314-327
65. ALICE Collaboration, “Measurement of charged jet suppression in Pb-Pb collisions at $\sqrt{s_{NN}}$=2.76 TeV”, Journal of High Energy Physics **03** (2014) 013
66. ALICE Collaboration, “Two and Three-Pion Quantum Statistics Correlations in Pb-Pb Collisions at $\sqrt{s_{NN}}$=2.76 TeV at the CERN LHC”, Physical Review C **89** (2014) 024911
67. ALICE Collaboration, “Technical Design Report for the Upgrade of the ALICE Inner Tracking System”, Journal of Physics G: Nuclear and Particle Physics **41** (2014) 087002